Journal Pre-proofs

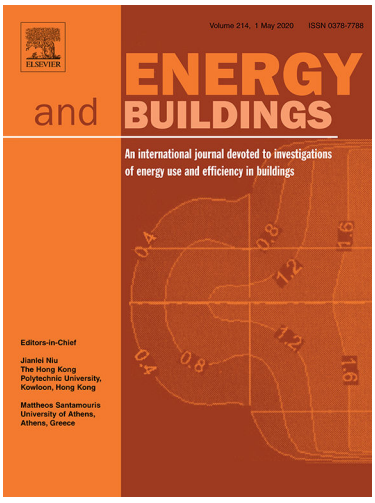

Design and development of lead-free glass-metallic vacuum materials for the construction and thermal performance of smart fusion edge-sealed vacuum glazing

Saim Memon, Philip C. Eames

PII: S0378-7788(20)32445-2
DOI: https://doi.org/10.1016/j.enbuild.2020.110430
Reference: ENB 110430

To appear in: *Energy & Buildings*

Received Date: 24 July 2020
Revised Date: 21 August 2020
Accepted Date: 27 August 2020

Please cite this article as: S. Memon, P.C. Eames, Design and development of lead-free glass-metallic vacuum materials for the construction and thermal performance of smart fusion edge-sealed vacuum glazing, *Energy & Buildings* (2020), doi: https://doi.org/10.1016/j.enbuild.2020.110430

Design and development of lead-free glass-metallic vacuum materials for the construction and thermal performance of smart fusion edge-sealed vacuum glazing

Saim Memon[1,2,*], Philip C. Eames[2]

[1] Solar Thermal Vacuum Engineering Research Group, London Centre for Energy Engineering, School of Engineering, London South Bank University, 103 Borough Road, London, SE1 0AA, UK

[2]Centre for Renewable Energy Systems Technology (CREST), School of Mechanical, Electrical & Manufacturing Engineering, Loughborough University, Loughborough, Leicestershire, LE11 3TU, UK

[*]Corresponding Author: Saim Memon

Address: Solar Thermal Vacuum Engineering Research Group, London Centre for Energy Engineering, School of Engineering, London South Bank University, 103 Borough Road, London, SE1 0AA, UK

Email: S.Memon@lsbu.ac.uk

Webpage: https://saimmemon.com

Tel: +44 (0)20 7815 7510

Abstract

Advancement in hermetic (vacuum-tight) edge-sealing materials has been one of the challenges since decades because of the existing cost, use of hazardous substance and complexity-to-construct issues in vacuum glazing. This paper presents novel experimental findings with designs and methods developed to construct and analyse thermal performance of the fusion edge-sealed vacuum glazing. The novel concept of fusion edge-seal consists of forming a thin glass-metallic rigid textured layer, in which the formation processes and experimental glass-metallic textured surface bonding property tests of 15 samples are microstructurally analysed using FIB-SEM and optical microscopy and succeeded the correct mixture of $B_2O_3$38-Sn62 wt%. Experimental analyses of at least 60 samples conducted using different techniques and Pb-free materials, among which five vacuum glazing samples of various designs and techniques discussed in this paper. The fusion edge-sealed vacuum glazing, constructed with bonded Sn62-$B_2O_3$38 wt% surface textured fused with Sn90-In10 wt% alloy at 450˚C, achieved at the hot-plate surface heat induction of 50±5˚C and the cavity vacuum pressure of $8.2 \cdot 10^{-4}$ Pa. Validated 3D FEM employed and the centre-of-sheet and total thermal transmittance values of fusion edge-sealed vacuum glazing (sample 'A5'), area of 300·300mm with 10 mm wide fusion edge-seal, predicted to be 1.039 and 1.4038 $Wm^{-2}K^{-1}$, respectively.

Keywords: energy-efficient vacuum glazing; lead-free glass-metal seal; materials design; energy conservation; finite element modelling; thermal performance

1. Introduction

The perception at which, nowadays, buildings cannot be imagined without glass is because glazed windows play an imperious role of allowing natural daylighting [1,2], but with repercussion of space-heating energy loss in cold-arid and space-cooling energy loss in hot-arid areas [3]. As such, evitable energy losses through glazed windows of buildings indirectly contributing to carbon emissions and, thus, impelling climate change [4]. This is, predominantly, due to an inadequate thermal transmittance value (U-value) of a glazing. In spite of the retrofits of a number of glazing technologies to building sector that usually do not compromise natural daylighting [5], such as cavity/cavities of two glass sheets (glazing) filled with air and/or heavy gases with low-e coatings, and could achieve the U-value of up to 1.4 $Wm^{-2}K^{-1}$ [6]; However, it does not account the increase of cavity thickness that affects window frame sizes and limits retrofit options on existing buildings. To achieve U-value of less than 1.1 $Wm^{-2}K^{-1}$ [7] without compromising the natural daylighting and cavity thickness, a vacuum glazing is a feasible solution [8]. Vacuum glazing has a 0.15 mm thick cavity between two sheets of glass, supported with an array of tiny stainless-steel pillars i.e. 0.15 mm high and 0.3 wide [9]. This cavity entails reduced atmospheric-air pressure down to high-vacuum pressure (between 0.13 Pa and $1.33 \cdot 10^{-4}$ Pa). Subsequently, it suppresses gaseous heat conduction and convection to infinitesimal level because of an increase of mean-free path between two air molecules beyond 3000 m. The high-vacuum pressure must be maintained with a hermetic (vacuum-tight) edge-seal around the periphery of two sheets of glass, whilst avoiding the problems of future gas leaks, outgassing and absorption of moisture in order to provide long-term durability. Thus, the U value is dependent on the vacuum-tight edge seal of the vacuum glazing.

Advancement in hermetic (vacuum-tight) edge-sealing materials is one of the challenges since decades because of the existing cost [10], use of hazardous substance (Pb) [11] and complexity-to-construct [12] issues in vacuum glazing that this paper addresses with empirical evidences. However, it is important to appreciate and briefly discuss the prior research art on the past inventions of vacuum glazing and discuss, here, the realism of the challenges exist the need of a new hermetic (vacuum-tight) edge-seal. The first successful construction of vacuum glazing [13] utilises the method of using Schott solder glass type 8467 (lead borate glass) [14] to hermetically seal the edges of two glass sheets at the high-temperature of around 450°C, this achieved the U-value of 0.8 $Wm^{-2}K^{-1}$ [15]. Subsequently, this method attained an attention at mass manufacturing level under the trade name ‘SPACIA’ in Japan by Nippon Sheet Glass (NSG) group [16]. It is often desirable to have lead (Pb)-free materials in building components, because the use of Pb is restricted in buildings and the allowable concentration quantity of not more than 0.1 wt % in homogeneous materials [17]. Though, the solder glass powder (Schott 8467) has more percentage of hazardous-substance (Pb) than regulated. This high-temperature solder glass edge-sealed vacuum glazing also impose restriction on the use of tempered glass and soft (low-emittance) coatings such as silver (Ag) [16]. The second successful construction of vacuum glazing utilises the method of ultrasonically soldering of pure indium 99.99% (In) around the periphery of two glass sheets at the low-temperature of around 156°C achieved U value of 0.86 $Wm^{-2}K^{-1}$ [18]. This method overcomes the restrictions of tempered glass and soft (low-emittance) coatings but inefficacious at the production level, because of the cost and scarcity of semi-precious metal (In). The third successful construction of triple vacuum glazing and vacuum glazing, invented by Dr Memon [19], was based on ultrasonically soldering the primary seal, at low-temperature around 200°C, made of composite CS-186 or Sn-Pb-Zn-Sb-AlTiSiCu in the proportion ratio of 56:39:3:1:1 by wt% and the secondary seal made of reinforced steel epoxy [20]. This composite hermetically sealed the edges of glass sheets and predicted the U-value of 0.33 $Wm^{-2}K^{-1}$ and 0.91 $Wm^{-2}K^{-1}$ for triple vacuum glazing and vacuum glazing, respectively. This method overcomes the cost issue, without compromising the scope of using tempered glass and soft coatings, but its composite edge seal has higher percentage of

lead (Pb) and it is complex-to-construct, mainly due to the need of precision in ultrasonically soldering the edges of glass sheets. The prior research methods have, however, quite successfully solved the problem of effective hermetic seal, design and construction improvements, fabrication processes and the significant predictions in the reduction of U value of less than 0.5 $Wm^{-2}K^{-1}$ for vacuum glazing units. But the current research challenges are the cost-effectiveness, not use of hazardous restricted metals such Pb, reduction in complexity-to-construct issue and the long-term stability of vacuum pressure in the cavity of the vacuum glazing.

It is perceptible from the above that there exists a need of the invention in the art for the development of an alternative cost-effective Pb-free edge sealing material for vacuum glazing, and corresponding novel method of making the same, including an improved evacuated cavity pressure with their stability over long term between opposing glass sheets.

To achieve hermeticity or vacuum-tight edge seal, a high vacuum pressure (0.13 Pa to $1.33 \cdot 10^{-4}$ Pa) is required in the cavity between two glass sheets supported by tiny pillars and must be maintained by the edge seal providing a mechanically strong bond, be free from gas molecules, match the thermal expansion characteristics between the glass and metals/alloys. It is, therefore, important to discuss, as follows, the (i) thermal expansion of sealing materials and glass; (ii) incidence of the interaction between glass and metal seal; (iii) importance of vapour pressure in choosing metals to form glass-to-metal seal and; and (iv) viscous behaviour of the glass and sealing materials.

1.1. Thermal expansion of glass-to-metal sealing materials

Glass-to-metal seals often have mismatch in their thermal expansion coefficients. This causes stresses and strains with uneven temperature distributions or contact with other metallic materials and composites [21]. To better match the thermal coefficients to the glass and the metal seal, an extra layer of different metal or layer of oxide could possibly produce the desired sealing composition [22]. The whole expansion characteristics of the sealing material (metal or solder glass) and the glass should also be considered [23]. For example, a certain amount of mismatch from 1 to $2 \cdot 10^{-7}$/˚C or even up to $6 \cdot 10^{-7}$/˚C (set-point temperature range of 300˚C to 600˚C) [24] could be tolerated in a solder glass to glass seal. Solder glasses are classified, according to their thermal expansion coefficients, into three categories: hard solder glasses with thermal expansion of $25 \cdot 10^{-7}$/˚C; semi-hard solder glasses with thermal expansion of 25 to $50 \cdot 10^{-7}$/˚C; and soft solder glasses with thermal expansion of more than $50 \cdot 10^{-7}$ /˚C [24, 25]. The thermal expansion of pure metals (such as Sn, Zn, Al, Cu, Bi, Pb or In) is linear with temperature, and that of its alloys the thermal expansion is linear up to the point of inflection. After which, their expansion increases more rapidly [26]. The solder glass seal becomes rigid, fragile, brittle and inelastic up to the inflection point and on further cooling to the ambient temperature. Substantial cracking in the solder glass bond will appear if the contraction rate of the glass and solder glass differs extensively [27]. A glass-to-metal seal could be under compressive stresses when the thermal expansion coefficient of metal is greater than the glass. The glass-to-metal seal is under tensile stress when the thermal expansion coefficient is less than the glass [24]. To substantiate stresses normal to the glass-to-metal interface, an approach suggested in [27] that when the metals of larger thermal expansion coefficient than the glass, the metal part needed to be soft and thin to deform elastically in order to allow changes in the dimensions of the glass when it cools. The total stress scenario in the glass-to-metal seal is far more complicated than in the case of fusion of different composition of materials to the glass surface. For the strong bond between solder glass and the glass, the thermal expansion coefficient of the solder glass must either be similar to or less than the glass.

In general, a good glass-to-metal seal can be achieved by either creating a layer of materials or interactions between the contact surfaces. The nature of the interaction and its mechanism vary dependent on the type of metal and/or its alloys. It was suggested in [28] that a good seal can be achieved when the glass is saturated with the appropriate metal oxide layer as a transitional character. At elevated temperature when the atoms of metal-wire and the metal ions of the soda-lime glass are moveable, because the chemical composition of soda-lime glass [29] has different weight % of SiO_2, Al_2O_3, TiO_3 and Fe_2O_3 and others. So, there will be a continuous exchange at the glass-to-metal interface. In an ideal case scenario for the formation of hermetic seal, metal ions from the soda-lime glass surface will diffuse into the metal-wire where they will gain electrons and become zero valence metal atoms. Whilst, the metal-wire atoms will diffuse into the soda-lime glass surface and become ionized. The reliability of the seal would then be assessed determined by thickness, uniformity and types of oxide layer [26]. The thickness of the layer is critical to avoid the oxide layer being porous or mechanically weak or brittle. In high vacuum applications, the presence of the oxide layer in the glass-to-metal seal should be avoided. Since, the seal enters into the outgassing processes such as surface desorption, diffusion and permeation of gases [30]. The surface appearance, such as colour change to a darker shade in the glass-metal after sealing, generally indicates the level of oxidation and the reliability of the seal. In some cases, however, e.g. tungsten, this is not a definite indication as to whether the seal contains or does not contain the required oxides. The level of oxidation is influenced by the type of metal used and the processing temperatures. Any gas molecules that remain trapped in the glass-to-metal seal usually form micro air gaps or pinholes in the seal. The processing temperature at which the oxide-layer is formed plays an important part in reducing oxygen molecules in the seal to a negligible level. For metals, if the surface is contaminated by a thin layer of oxide, the initial outgassing rate at ambient temperature is of the order of 10^{-4} Pa m^3 $s^{-1}m^{-2}$ [26]. Nevertheless, the outgassing rate decreases with time and subject to temperature regimes applied. The rate of outgassing increases due to the presence of water vapour between the seal and the glass. This can be decreased exponentially to a much lower value by continuing evacuation for more than 10 hours. The gases left within the seal are commonly CO, CO_2, O_2, N_2 and H_2 which can be removed during the molten stage of the seal [21] by making it under high-vacuum environment. Some of these gases react with metals to form compounds. The type and composition of the materials used for sealing and the cleaning methods used before fabricating the sample will determine the gases that are left.

1.3. Importance of vapour pressure in choosing metals to form a glass-to-metal seal

The vapour pressure of metals indicates the evaporation rate in the liquid phase and is a tendency of molecules in a liquid phase, at a given temperature, to escape within a closed system. For example, the vapour pressure of In increases from 10^{-2} Pa to around 1 Pa with a temperature increase from around 650˚C to 850˚C. Comparing this with Sn for a similar temperature increase, the vapour pressure increases from 10^{-5}Pa to $8{\cdot}10^{-3}$Pa. At ambient temperatures metals, such as Pb, In, Sn, Bi, Sb, Zn, or Cd, have a vapour pressure above 10^{-9} Pa [21]. Among these metals, Cd and Zn have a higher vapour pressure and should be avoided, and not as elements for the formation of glass-metal seals. Pb, Sn and In can be used in high vacuum applications due to their low vapour pressures [26, 31]. Bi is brittle in nature and individually this element cannot be used in high vacuum applications for the glass-metal seals [32]. The basis of the method and techniques explored in this research is the use of B_2O_3 to form a layer of oxides on the glass surface, which become glassy and rigid in shape after heating to its melting temperature. It is worth noting that the formation of B_2O_3 was initially reported in the scientific paper no. 857 from research laboratories of Westinghouse Electric & IC manufacturing company in 1937 and then patented in [33]. B_2O_3 has

increasing applications as a fluxing agent for glass and enamels [34]. The melting point of crystalline B_2O_3 is between 450˚C and 470˚C.

1.4. Viscous behaviour of the glass-to-metal sealing materials

One of the essential characteristics, when forming a glass-to-metal seal, is the viscous dynamic behaviour at their straining and setting point. In addition to the thermal expansion of the materials, the viscosity at melting temperature of the material also influences the mechanical rigidity of the seal. According to the ASTM definition [35], glass is an inorganic liquid product which has cooled off and solidified, with very high viscosity, without crystallizing. When the temperature increases, the viscosity decreases and the glass gradually assume the character of a liquid. Glasses are traditionally classified into two categories. The first category is the 'hard' or borosilicate, in which the main additive to the silica is B_2O_3. The second category is the 'soft' in which the main additive is either Na_2O to give soda glass or PbO to give lead glass [21]. At the temperature of 470˚C [27] when all movement of the glass molecules at which a certain glass viscosity is reached and no more strain can be introduced into the hot soda glass (strain point) the viscosity is $\approx 10^{13.5}$ Pa.s [21]. The viscosity of 10^{14} Pa.s [36] is believed to be the limit for the solid (fragile) body of the glass. For temperatures above 300˚C, a tempered glass begins to lose its temper and because of this it could not be used for the high temperature construction process. Glasses with low softening temperatures (<600˚C) are often referred to as solder glasses. In general, the set point temperature of the glass to solder glass seal is ≈ 510˚C. In which the viscosity of the glass being $\approx 10^{12}$ Pa.s and the viscosity of solder glass is in between 10^4 and 10^5 Pa.s [26]. The pure metals or alloys of In, Sn, Bi or Pb, the viscosity is above 10^{14} Pa.s can be achieved at the temperature less than the strain point of the glass, this could be the fragile or solid phase point i.e. below 350˚C [27].

The concept of producing alloys for the glass seals has, however, offer a number of solutions. An alloy of Bi (53-76 wt %), Sn (22-35 wt %) and In (2-12 wt %) was claimed to have an excellent oxidation resistance and sealing property suitable for rotating plug of a nuclear reactor [37]. Pb-B glasses or Pb-Zn-B glasses in which the Zn-Pb (mol ratio below 1:2) was claimed to be used in sealing semiconductor packages at the temperature of 450˚C [38]. A glass solder consists of B_2O_3 (20-30 mole %), PbO (60-69 mole %), ZnO (0-10 mole %), CuO (0-6 mole %) and Bi_2O_3 (0.5-2.0 mole %). In which the mixture of these composites with SiO_2 and Al_2O_3 could be a suitable solution to seal with soda-lime-silica glass [39]. A lead-free composite material or a glass sealing paste consists of Bi_2O_3 (70-90 wt %), ZnO (1-20 wt %), B_2O_3 (2-12 wt %), Al_2O_3 (0.1-5 wt %), CeO_2 (0.1-5 wt %), CuO (0-5 wt %), Fe_2O_3 (0-0.2 wt %) and CuO+Fe_2O_3 (0.05-5 wt %) was claimed to be a reasonable sealing composite for the glass seal [40].

To date, there has been no reported study which has identified a cost-effective, Pb-free and ultrasonic-soldering free high temperature sealing method for vacuum glazing construction and to triumph these challenges, this paper presents the novel experimental findings that addresses these issues. In this paper the design, methods and techniques to form a hermetic edge seal, named as a fusion edge-seal, are presented for the successful construction of fusion edge-sealed vacuum glazing. Fusion edge-seal is constructed with a process invented after a series of experiments that involves the formation of the a thin glass-metallic surface texture, made of the particles of B_2O_3 and/or Sn, and successfully fused with the hard Sn or Sn-In alloy to form an hermetic (vacuum-tight) edge-seal. This requires the formation of a textured layer on the glass surface using an appropriate mix of B_2O_3 and/or Sn. This method, as shown in Fig. 1, was achieved after detailed study and experimentations in understanding the glass components and metals behaviour at different temperature regimes. This paper also contributes to the thermal performance prediction of the fusion edge-sealed vacuum glazing with a validated finite element model of the fabricated (sample 'A5').

One of the main drifts of this invention is its cost-effectiveness, if compared to composite or indium sealed vacuum glazing, discussed in this paper, and it doesn't contain any hazardous Pb metal in it which compared to solder glass sealed vacuum glazing. Other features and advantages of the fusion edge-seal will become apparent upon examining the following detailed experimental analyses of the fusion edge-sealed vacuum glazing.

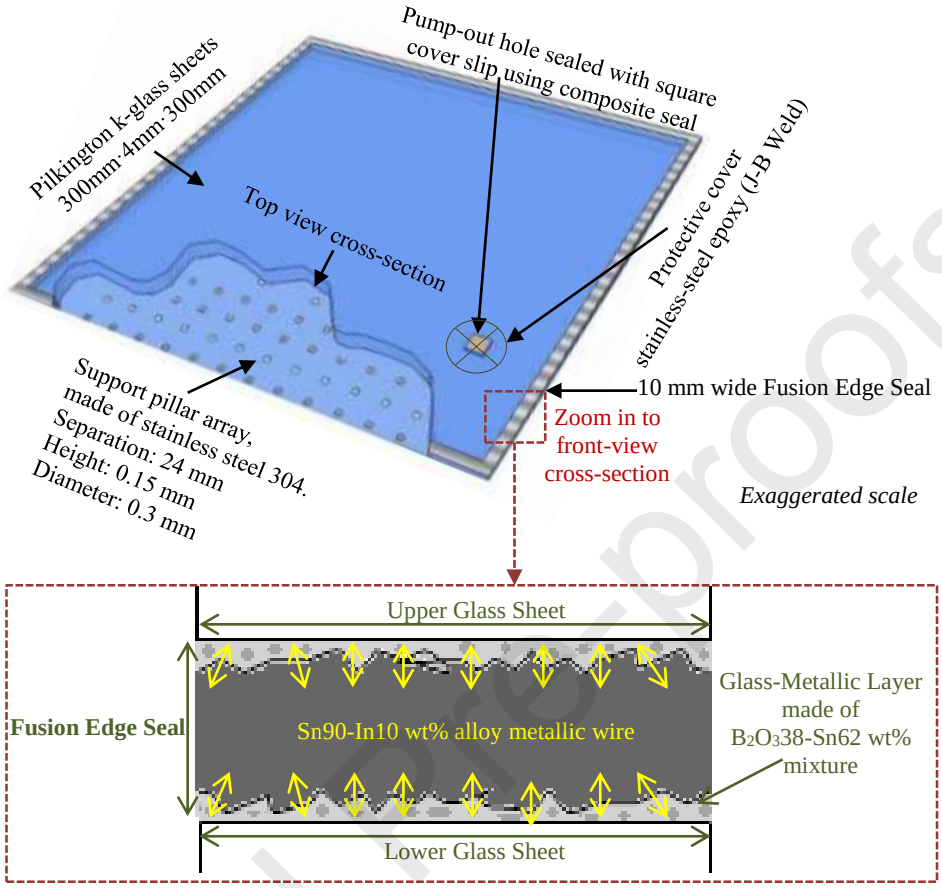

Fig. 1. A schematic diagram of novel fusion edge-sealed vacuum glazing constructed with bonded Sn62-$B_2O_3$38 wt% mixture for surface texture fused with Sn90-In10 wt% alloy at high-temperature.

2. Experimental methodology on constructing the fusion edge-sealed vacuum glazing

An overview of the systematic approach employed performing theoretical and experimental analyses for the construction of fusion edge-sealed (high temperature hermetic edge-sealed) vacuum glazing units are summarised in the block diagram in Fig. 2, details are also available in the dataset [43]. The first part was to experimentally investigate the soda-lime and borosilicate glass components. The second part was to study the complexities in the interaction of a glass with metals and solder glasses. The third part was to construct vacuum glazing samples to choose materials and develop novel composites. It is often desirable to have lead-free materials in building components and to utilise higher weighted % of Sn. The reason of using an alloy of higher Sn wt% for the formation of hermetic glass edge-seal is due to, but not limited to: the abundance of Sn, i.e. 2ppm in the earth's crust, is higher than In, i.e. 0.122ppm [41,42]; and to avoid the use of Pb which is restricted in buildings and the allowable concentration quantity of not more than 0.1 wt% in homogeneous materials [17], though the solder glass powder (Schott 8467) [15] has more percentage of Pb than regulated.

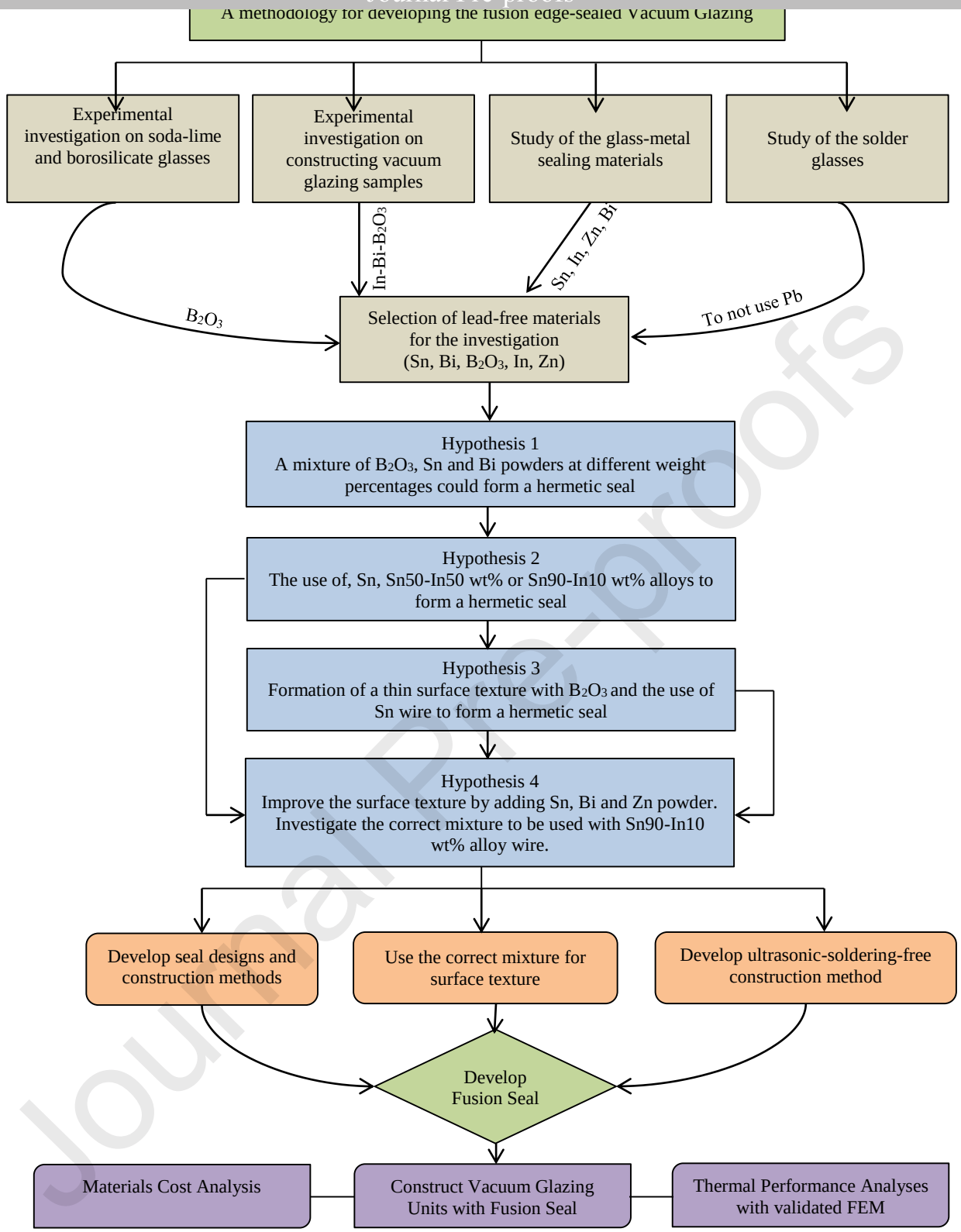

Figure 2: An overview of the systematic approach employed for the development of fusion edge-seal (high temperature hermetic edge seal) for the construction of vacuum glazing units.

Thus, five Pb-free materials were selected that are Sn, Bi, B_2O_3, In and Zn for the investigation to develop a new high temperature based edge-sealing material. The first hypothesis developed was to use B_2O_3, Sn and Bi powders at different weight percentages. With this, initially, a number of samples were constructed in which all of the edge seals were porous and brittle. The second hypothesis was to use Sn wire and alloys of Sn50-In50 wt% alloy and Sn90-In10 wt% alloy for the formation of a seal with the k-glass. But these were

having inadequate thermal expansion match, eventually produces mechanically weak bond. The third hypothetical idea developed was to form a surface texture with B_2O_3 and the use of Sn wire to be melted on to the surface texture at temperature of 450˚C. The reason a surface texture idea was invented was to create an incidence of the interaction between glass and Sn or Sn90-In10 wt% alloy forming a thin glassy layer. The fourth hypothesis was to improve the surface texture by adding or removing Sn, Bi and Zn powders to form a correct mixture which should be rigid and be able to make a hermetic bond with Sn90-In10 wt% alloy wire. Subsequently, the concept of forming novel fusion edge-seal was evolved to create a thin glass-metallic layer, using an appropriate admixture of B_2O_3-Sn, as an incidence of the interaction between a soda-lime glass surface and an alloy of higher Sn wt%, fused at different temperature regimes. This requires the formation of a textured layer on the glass surface using an appropriate mix of B_2O_3 and Sn. From a molecular point of view, the interaction of glass-to-metal occurs in a transitional region when the Sn90-In10 wt% alloy wire gradually forming an ionic-covalent fuse with the textured surface forming a thin glassy layer. This method was achieved after several experimental investigations and the study of the glass components and metals behaviour at different temperature regimes which are detailed in the following sections.

3. Microstructural analysis on the formation of thin glass-metallic surface textured layer

The concept of forming a thin textured layer on the surface of a glass sheet is presented in this section. Initially, two materials were studied to produce the textured layer. Fig. 3a shows an illustration of a texture layer of (B_2O_3) and Fig. 3b shows an illustration of a texture layer of admixture of B_2O_3 and Sn/alloys particles.

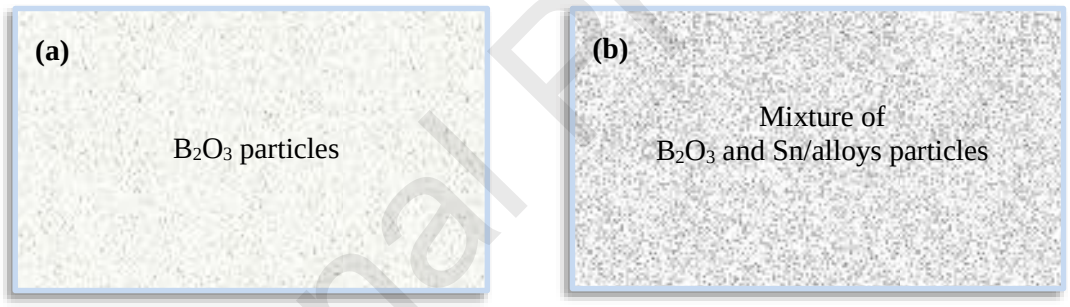

Figure 3: (a) Illustration of textured surface produced from crystals of B_2O_3, and (b) textured surface produced from admixture of B_2O_3 and Sn/alloy particles. *(Not to scale)*

Treatment with B_2O_3 is considered advantageous in the formation of glass-metal seal. Due to the phase transitions of B_2O_3, glassy crystals to disordered condensed liquid form, when heating to 450˚C followed by then formation of a hard-glassy discontinuous rigid shape on the glass surface. The concept of introducing a metal powder to the crystals of B_2O_3 to improve the viscous behaviour is investigated. This may result when B_2O_3 molecules react with metal atoms when both are in the liquid state. In this study, the powdered metals studied were Sn, Bi and Zn combined the mixture with B_2O_3.

In order to arrive at the correct mixture of B_2O_3 and powdered metals (Sn, Zn, Bi and/or their combinations) and/or the use of Sn-steel-Sn sheet for the formation of a suitable texture surface and subsequent fusion seal, more than 25 samples were fabricated from which 15 samples are presented here. In which the materials at different wt% were tested to understand and achieve the rigid texture surface and/or to be able to achieve a thin glassy layer between glass and metal wire to form a hermetic seal. These are listed in the Table 1.

The samples in Table 1 were made in two environments, one being exposed condition in which the samples were prepared on a hot plate i.e. samples 'EA', 'EB' and 'EC'. The other being closed conditions in which the samples were prepared inside an oven i.e. 'C-1', 'CA', 'CB', 'CC', 'CD', 'CE', 'CF', 'CG', 'CH' and 'C-2'. The reason of choosing two conditions was to understand the behaviour of the composites under uniform air temperature and non-uniform air temperature (a use of hot-plate surface heat induction).

The specific temperature profile method was developed after a number of sample constructions in which approximate temperature regimes used, as shown in Fig. 4. In the first heating phase, the temperature was increased to 300˚C. The melting temperatures of pure Sn, Bi and Zn are 231.93˚C, 271.5˚C and 419.53˚C, respectively. The Zn powder was employed due to its wider applications in alloys for producing the rigid bonds with glass. The percentage weight used was not more than 7.5 wt% of Zn powder. In the second heating phase, the temperature was held at 300˚C for 20 minutes to let the metal powder, Sn and/or Bi, melt. In the third heating phase, the temperature was increased to 450˚C and then held at this temperature for 30 minutes. This allowed the molten metal powder or metal-alloys to react with the molten B_2O_3. In the fifth heating phase, the sample was steadily cooled down to the ambient temperature of 21˚C, this is because the cooling process may introduce stresses on the sealing area, due to the difference in thermal expansion of glass and metal/alloy, if not gradually cool the sample down to an ambient temperature.

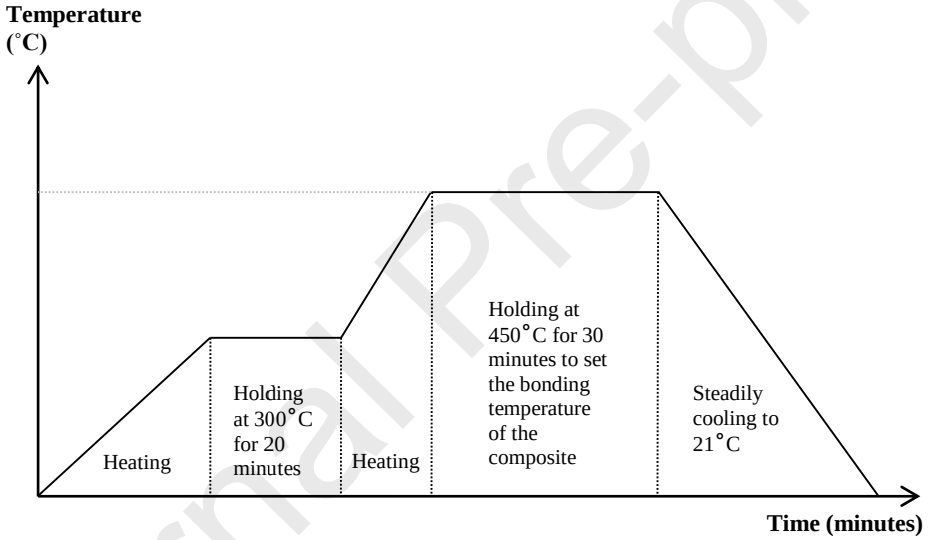

Fig. 4. Heating regime used for the formation of a textured glass surface under the enclosed and exposed environmental conditions.

The textured surface property was classified into three types:

- A 'good' sample is characterised by a rigid textured surface with no apparent porosity or brittleness in the surface.
- An 'acceptable' sample represents a surface that has little apparent porosity and brittleness in the structure.
- A 'fail' sample indicates a porous and brittle surface with poor oxidation resistance evidenced by colour changing.

The classification of the textured surfaces is given in Table 1. The materials surface condition, after bonding to the SnO_2 coated surface of the k-glass, of selected samples from Table 1 are then critically analysed and discussed by using focus ion beam scanning electron microscope (FIB-SEM) and optical microscope to select the most promising mixture from the materials tested for formation of the fusion edge-seal as shown in Fig. 5. From Table 1, all of the alloys used are Pb-free. The most promising criteria for

selecting the correct mixture were: to micro-structurally analyse the seal and a creation of a thin glassy layer, and to test the surface texture with metal/alloy wire at high temperature, by evacuating the sample. This idea was based on the hypothesis developed by experimentations on materials for over three years.

Table 1
Details of the mixtures used in the formation of glass surface texture suitable for fusion bonds ranking of the surface texture characteristics.

Sample No.	Type	Proportion Weight %					Quantity	Sealing	Fig.
		B_2O_3	Sn	Bi	Zn	Sn-Steel-Sn (0.2mm sheet)	Grams	Property	No.
1	'C-1'	100	-	-	-	-	0.3	Good surface texture	-
2	'CA'	39.3	60.7	-	-	-	0.5	Acceptable surface texture	-
3	'CB'	10	90	-	-	-	0.5	Fail	-
4	'CC'	20	50	30		-	0.5	Acceptable surface texture	5a
5	'CD'	35	50	7.5	7.5	-	0.5	Fail	5b
6	'CE'	5-7	93-95*	-	-	-	2	Acceptable for bonding	
7	'CF' (correct mixture)	38	62	-	-	-	0.5	Good for the bond and the surface texture	5c
8	'CF'-(repeat)	38	62	-	-	-	0.5	Good for the bond and the surface texture	5d
9	'CF' (fusion sealed sample)	38	62	-	-	-	0.5	Good for the bond and the surface texture	5e
10	'CG'	36	64	-	-	-	0.5	Acceptable for the surface texture and for the bond if a copper gasket wire used	5f
11	'CH'	25	58	7.5	7.5	-	0.5	Acceptable for the surface texture	-
12	'EA'	1-1.5	2-3.5	-	-	95-97	0.72	Acceptable for the bond if fabricated in a controlled radiative heating environment	5g
13	'EB'	35	65	-	-	-	0.5	Acceptable for the surface texture	5h
14	'EC'	35	50	7.5	7.5	-	0.5	Fail	5i
15	'C-2'	38	62	-	-	-	0.1	Successfully created the textured thin layer on the glass surface	5j

C= The sample made under enclosed environment in the radiative heating oven
E=The sample made under open environment on the hot plate
* Purity of 99.999% of tin (Sn) solder wire

The sample 'C-1' was formed with B_2O_3 (crystals grain size of ≈ 74 microns) heated to 450˚C on the glass surface. The B_2O_3 crystals formed a glassy rigid textured shape on the glass surface. This was considered to be a 'good' sample and a useful material for the formation of surface bonds.

It was hypothesized that the addition of metal powders to the crystals of B_2O_3 could possibly achieve a better textured surface. Sample 'CA' was fabricated with a mixture of B_2O_3 and Sn (grain size of smaller than 44 microns) having a proportion of 39.3 wt% and 60.7 wt%, respectively. This found to be 'acceptable' for the creation of a surface texture due to the rigidity of the surface formed. Some of the crystals of B_2O_3 and Sn did not melt together due to the mismatch in the wt%.

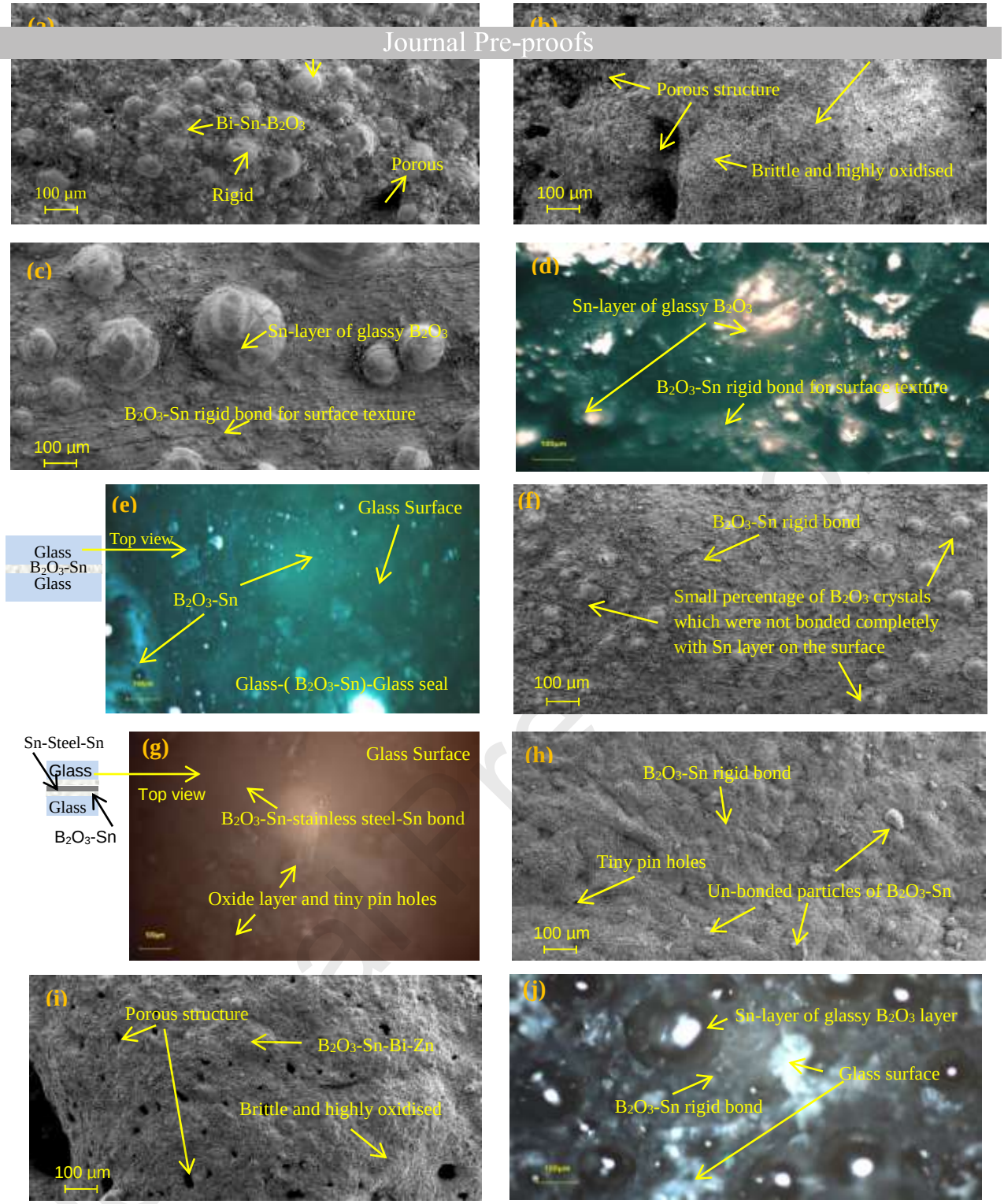

Figure 5: (a) FIB-SEM of sample 'CC' formed with B_2O_3-Sn-Bi at ratio of 20:50:30 wt%, (b)FIB-SEM of sample 'CD' formed with B_2O_3-Sn-Bi-Zn at ratio of 35:50:7.5:7.5 wt%, (c) FIB-SEM of sample 'CF' formed with B_2O_3-Sn at ratio of 38:62 wt%, (d) optical micrograph of sample 'CF' formed with B_2O_3-Sn at ratio of 38:62 wt%, (e) optical micrograph of sample 'CF' bond formed with B_2O_3-Sn at ratio of 38:62 wt%, (f) FIB-SEM of sample 'CG' formed with B_2O_3-Sn at ratio of 36:64 wt %, (g) optical micrograph of sample 'EA' fabricated with a 0.2mm thick Sn-steel-Sn sheet proportion of 95-97 wt% with textured layer made of Sn-B_2O_3 at ratio of 1-1.5 wt% and 2-3.5wt% respectively, (h) FIB-SEM of sample 'EB' formed with B_2O_3-Sn at ratio of 35:65 wt%, (i) FIB-SEM of sample 'EC' formed with B_2O_3-Sn-Bi-Zn alloy at ratio of 35:50:7.5:7.5 wt%, and (j) optical micrograph of sample 'C-2' formed with a mixture of $B_2O_3$38-Sn62 wt%, the same mixture as used in sample 'CF', showing the formation of a rigid and hard thin textured layer on the glass surface.

The sample 'CB' was formed to investigate the influence of reducing the B_2O_3 wt%. The mixture used was 10 wt% of B_2O_3 and 90 wt% of Sn. The sample 'CB' mixture 'failed' with a poor surface formed thus was insufficient wt% of B_2O_3.

The sample 'CC' was formed with B_2O_3-Sn-Bi in the proportion ratio of 20:50:30 by wt%, respectively. The surface formed was analysed, using the Focus Ion Beam Scanning Electron Microscopic (FIB-SEM) system, and found to be 'acceptable' providing a rigid surface structure. This was, however, not considered suitable for the development of a fusion edge-seal due to its porous structure, as illustrated in Fig 5a.

The sample 'CD' was formed using B_2O_3-Sn-Bi-Zn having proportions of ratio 35:50:7.5:7.5 by wt% respectively. This sample was classed to 'failed'. The surface structure formed was porous, highly oxidised and exhibited colour change to slight black, as can be seen in the FIB-SEM image in Fig. 5b.

The sample 'CE' was formed with crystals of B_2O_3 and with pure Sn wire having approximate proportions of 5-7 wt% and 93-95 wt% respectively. This formation approach was observed to be 'acceptable' for the development of a fusion edge-seal due to its rigidity, consistency and the non-porous nature of the surface texture.

The sample 'CF' was fabricated with B_2O_3-Sn alloy having proportions of ratio 38:62 by wt% respectively. This composite mixture was analysed and found to be 'good' for the textured surface and suitable for the formation of a rigid textured composite surface and for the fusion edge-seal. This was due to the formation of a glassy B_2O_3 layer on the Sn surface. This successful experiment was repeated and the same composite mixture was applied and used to bond two pieces of k-glass together. As illustrated in the FIB-SEM image in Fig. 5c and the optical microscope image Figs. 5d and 5e. Although, impurities may be contained in the $B_2O_3$38-Sn62 wt% alloy due to the formation of the surface texture in the non-clean environment inside the oven.

A slight variation in the mixture of the 'good' sample 'CF', gave sample 'CG' fabricated with B_2O_3-Sn composite having proportions of ratio 36:64 by wt% respectively. This mixture was analysed and found to be 'acceptable' in the formed textured surface due to its rigidity and consistency. However, compared to sample 'CF', this mixture was not considered suitable for forming a fusion seal, as can be seen in the FIB-SEM image in Fig. 5f.

The sample 'CH' was formed with B_2O_3-Sn-Bi-Zn having proportions of ratio 25:58:7.5:7.5 by wt% respectively. This was achieved with the slight variation in the B_2O_3-Sn composition of sample 'CD'. This was considered to provide an 'acceptable' textured surface but not be suitable for fusion edge-seal due to the presence of zinc powder that did not appear to be bonded to the B_2O_3.

The sample 'EA' was designed with B_2O_3-Sn mixture and a Sn-steel-Sn 0.2mm thick sheet having approximate proportions of 1-1.5 wt%, 2-3.5 wt% and 95-97 wt%. This combination of the textured surface of B_2O_3-Sn alloy and the sheet of Sn-steel-Sn gave promising results, as can be seen in Fig. 5g. This is due to the seal structure formed being rigid, non-porous, and mechanically strong. This idea/method was not repeated further or pursued due to the formation of minute pin holes and an oxide layer.

The sample 'EB' was formed using a mixture of B_2O_3-Sn ratio of 35:65 by wt%. The surface formed was analysed, using a FIB-SEM, and found to be 'acceptable' in terms of surface texture only. It can be seen,

from Fig. 5h, that un-bonded crystals of B_2O_3-Sn and tiny holes are present on the surface; despite the fact the structure was rigid and mechanically strong, it was not good for the formation of a fusion edge-seal.

As noted, sample 'CD' was classified failed, sample 'EC' had a similar mixture of materials but was formed on the hot plate. From Fig. 5i, FIB-SEM image of the surface formed this mixture (B_2O_3, Sn, Bi, Zn ratio of 35:50:7.5 by wt% respectively) does not form an acceptable surface texture. The surface structure was found to be porous, brittle, highly oxidised and exhibited colour change to a slight black. The formation of a textured surface on the hot plate (exposed condition-E) is not recommended. The use of an oven was more successful in achieving a good textured surface due to a uniform air temperature.

After achieving repeated positive results for the mixture used for sample 'CF', a thin textured layer on the k-glass was formed. The sample 'C-2' surface formed was rigid, as seen in the optical micrograph image Fig. 5j. This textured surface was used to form the basis of the successful fusion edge-sealed vacuum glazing.

4. Fusion seal design and construction processes for vacuum glazing

In the following sub-sections only five vacuum glazing sample designs and construction processes are reported. These samples are named 'A1', 'A2', 'A3', 'A4' and 'A5'. The reason to present the details of these samples is to validate the refined experimental design and construction process achieved for the novel development of fusion-sealed vacuum glazing (sample 'A5').

4.1. Sample 'A1': Design and construction process

The three-stage design process for the construction of sample 'A1' (area of 150mm·150mm) was developed, and was based on the bond developed in sample 'C-1', as illustrated schematically in Fig. 6a. In which, the first stage was to produce a fine powder (≈ 74 microns) of B_2O_3 crystals and deposit them consistently on the edge of the glass surface followed by heat at 450˚C in an oven to form a rigid textured surface. The second stage was to ultrasonically solder pure Sn wire on to the textured surface with an addition to positioning two Sn wires (1 mm in diameter) on the sealing area and lowering the top glass sheet on to the bottom sheet. The reason to add Sn wires on top of the soldered Sn on textured surface was to avoid the risk of micro-gaps on the rough soldered Sn surface. The third stage was to place the two glass sheets together, separated by the support pillars inside the oven and then use the heating regime illustrated in Fig.4. The high-vacuum system with vacuum cup for the evacuation and sealing of the pump-out hole was utilised, details are reported elsewhere by Memon *et al* (2019) [12].

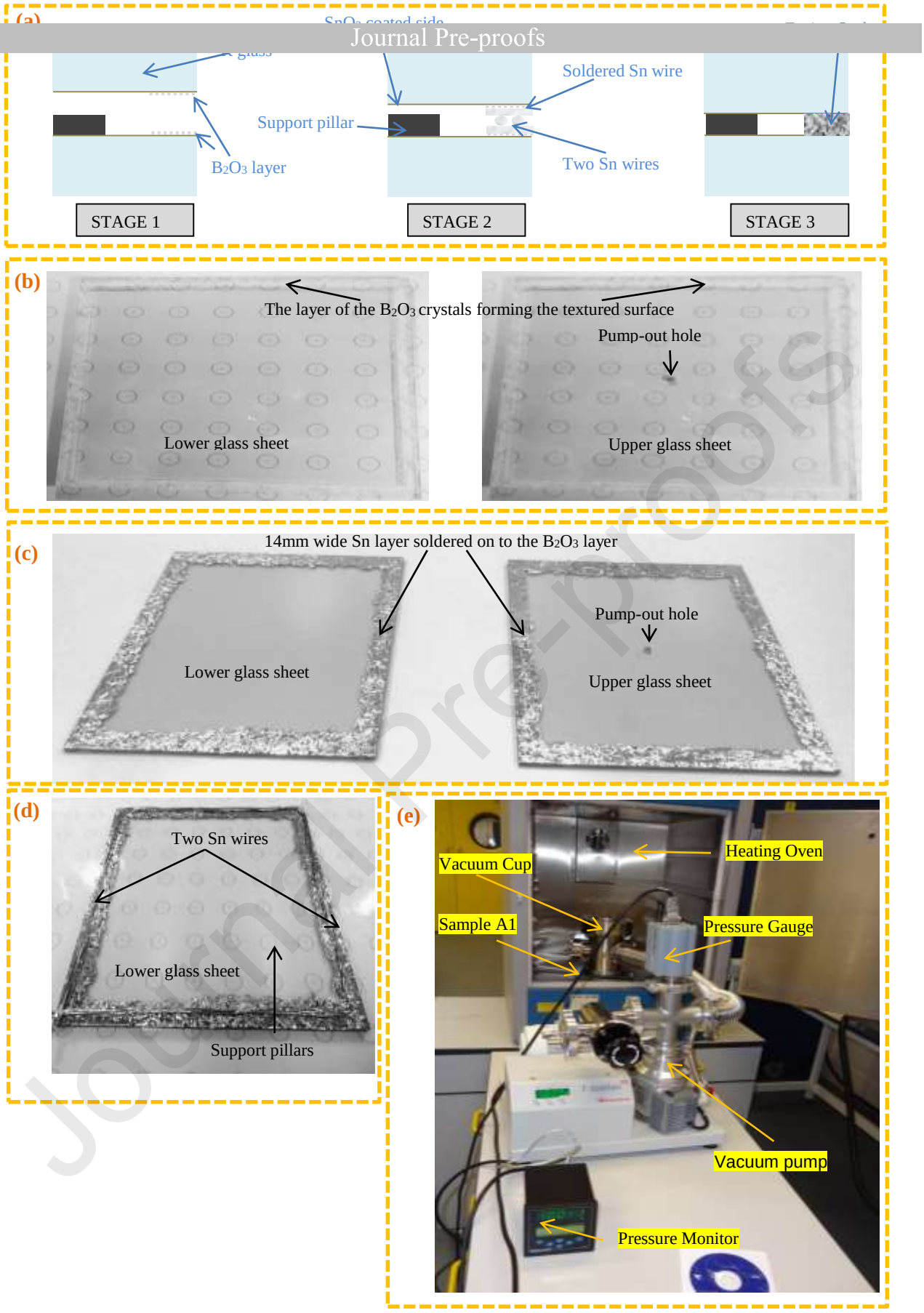

Fig. 6. Shows (a) three stage design process for sample 'A1', (b) the layer of the B_2O_3 crystals forming the textured surface, (c) ultrasonically soldered Sn around the periphery of two glass sheets, (d) two Sn wires were placed on top of the soldered edge area of the lower glass sheet, and (e) experimental setup for the evacuation using high-vacuum system for sample 'A1' in the low temperature (≈110˚C) heating oven.

The detailed construction process implemented for sample 'A1' is as follows:

(i) Two Pilkington k-glass sheets were sliced to the size of 150·150·4mm. A pump-out hole (4mm in diameter) was drilled in a sheet of upper glass for evacuation located at 75 mm from two corner edges. The glass sheets were cleaned with water, isopropanol and acetone.

(ii) A fine powder of crystalline B_2O_3 (≈ 74 microns), was prepared using a mortar and pestle, and deposited at the width of 14mm on the edge of the glass surface. It was heated at 450˚C to form a rigid textured surface, as it can be seen in Fig. 6b. In addition to the formation of the textured surface, the glass sheets were additionally baked-out at 120˚C to remove moisture from the glass surface.

(iii) The edge sealing material, in this case pure Sn wire was applied by ultrasonically soldering the Sn around the periphery of two glass sheets on to the B_2O_3 rigid textured surface, as shown in Fig. 6c.

(iv) Stainless steel support pillars (0.15 mm in height and 0.3mm in diameter) were positioned on the lower glass sheets in a square array of pitch 24mm with each other.

(v) The two Sn wires were placed on top of the soldered edge sealing area of the lower glass sheet, as shown in Fig 6d. The upper glass sheet was lowered on to the support pillars and edge seal.

(vi) The sample was heated in an oven to 450˚C following the heating regime, as shown in Fig. 4.

(vii) The sample was placed in a low temperature heating oven and heated to a rough heating environment (≈110˚C) for the evacuation using the vacuum cup, as shown in Fig 6e.

4.2. Sample 'A2': Design and construction process

The sample 'A2' (area of 150mm·150mm) was designed replacing the Sn wire with Sn90-In10 wt% alloy wire to enhance the bond with B_2O_3 textured surface. The design process has three stages implemented for construction, as illustrated schematically in Fig 7a. In which, the stage one was identical to sample 'A1' in section 4.1. The second stage was to ultrasonically solder the Sn90-In10 wt% alloy wire on to the B_2O_3 rigid textured glass surface as shown in Fig 7b, in addition to positioning one Sn90-In10 alloy wt% wire (2mm in diameter) on the edge sealing area as shown in Fig. 7c. The third stage was to place the two glass sheets together, separated by the support pillars inside the oven to heat, in a similar arrangement to sample 'A1'. During evacuation the pump-out hole was sealed by heating the Cerasolzer alloy (CS-186) coated glass square using the cartridge heater in the vacuum cup.

4.3. Sample 'A3': Design and construction process

The sample 'A3' (area of 150mm·150mm) was designed without using ultrasonic-soldering Sn90-In10 wt% alloy wire. The reason to not use ultrasonic-soldering method is to save the electrical energy consumption, time, laborious work and simplifying the production process for vacuum glazing. This was based on the B_2O_3 textured surface and Sn90-In10 wt% alloy wire to join the two sheets of glass. The design process for sample 'A3' has three stages implemented for construction, as illustrated schematically in Fig. 8a. In which, the stage one implemented was identical to sample 'A1'. The second stage was to place Sn90-In10 wt% alloy wire on the B_2O_3 rigid textured edge sealing area and lower the top glass sheet on to the bottom sheet. The third stage implemented was identical to sample 'A2' in section 4.2. In this construction process, the evacuation of the sample 'A3'was performed by placing it on a hot plate and heated to maximum of 150˚C, as shown in Fig 8b.

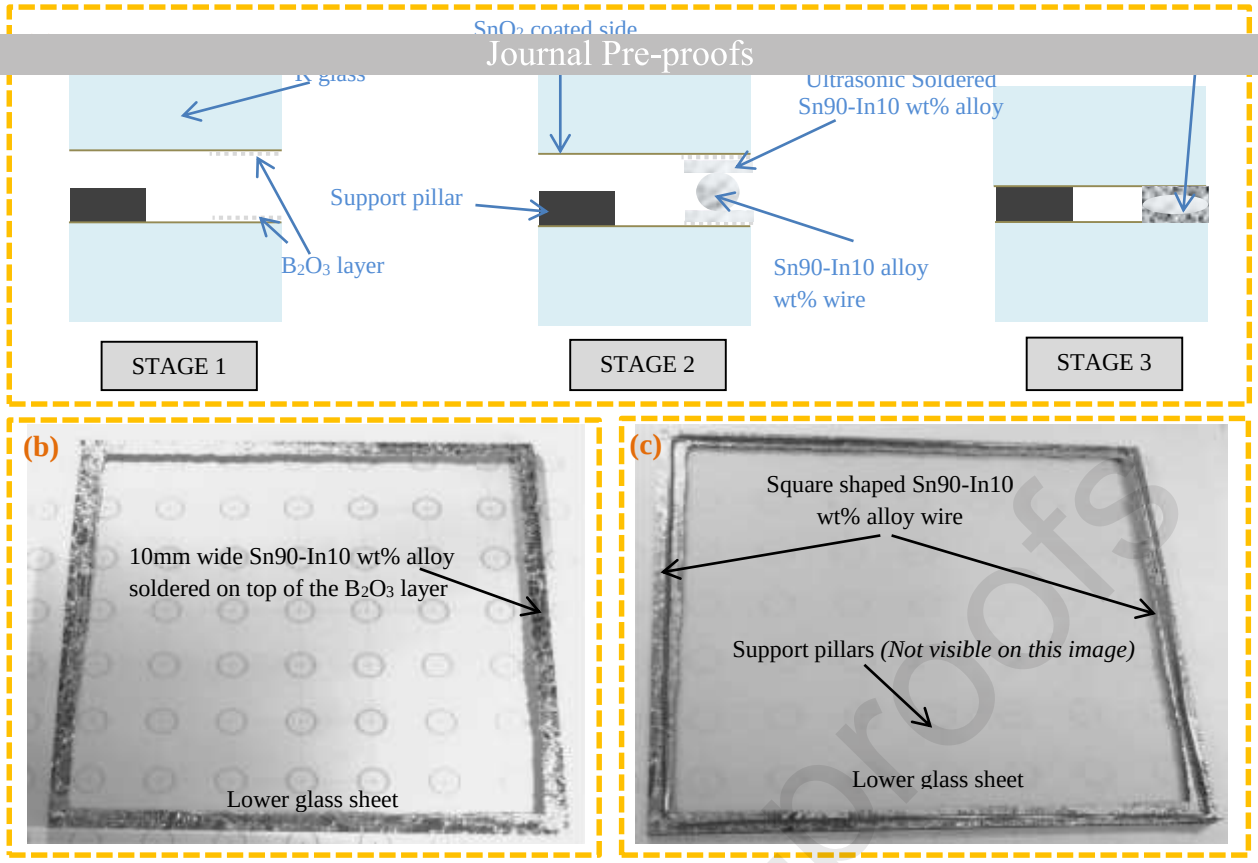

Fig. 7. Illustrates (a) three stage design process for sample 'A2', (b) 10 mm wide Sn90-In10 alloy wt% soldered on top of the rigid B_2O_3 textured surface, and (c) positioned square shaped (2 mm diameter) Sn90-In10 alloy wt% wire on the sealing area.

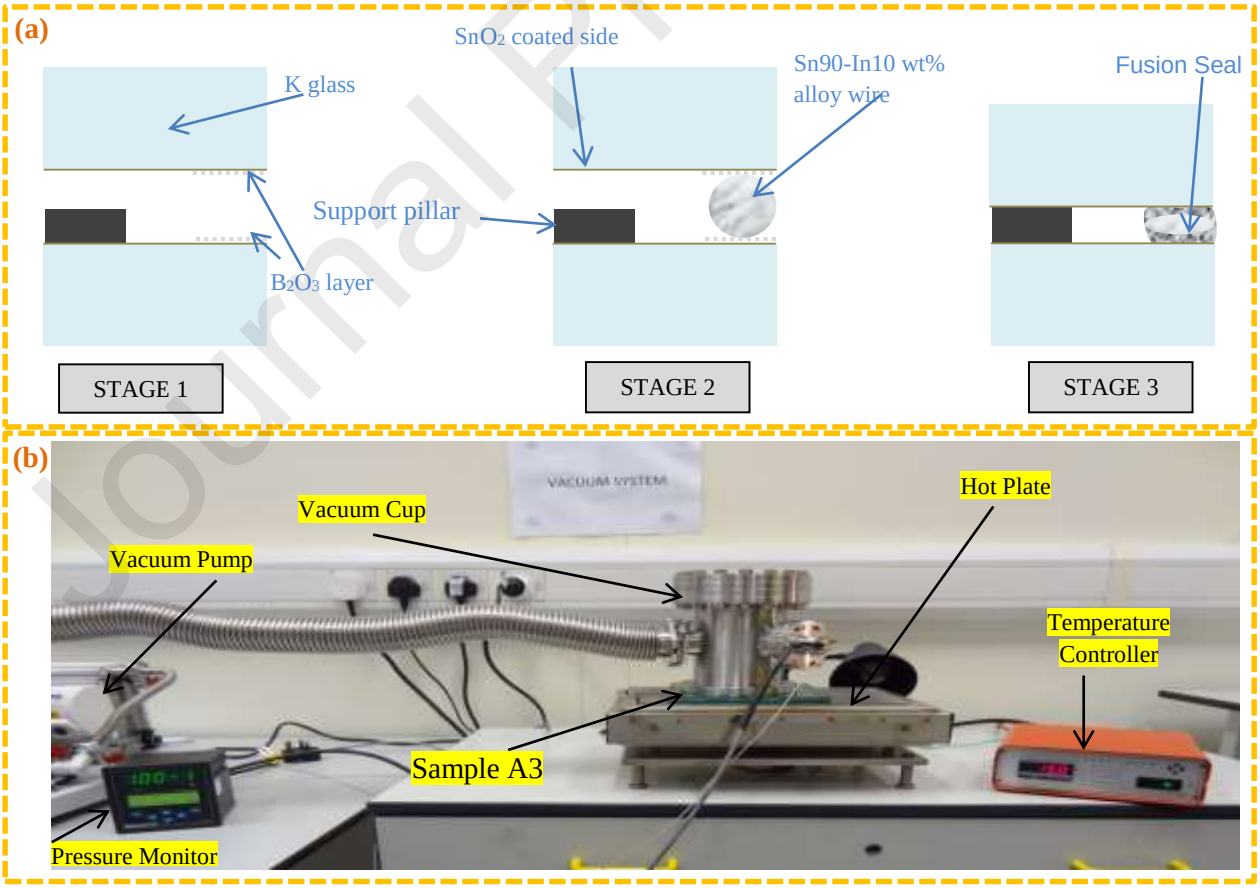

Fig. 8. Illustrates (a) three stage process for sample 'A3', similar to that of 'A2' with no ultrasonic soldering, and (b) experimental setup for evacuation of sample 'A3' using a hot plate with a maximum surface induction temperature of 150˚C.

4.4. Sample 'A4': Design and construction process

The sample 'A4' (area of 170mm·170mm) used similar materials to those used in sample 'A3'. In this trial, the seal design was improved by forming a thin texture layer of B_2O_3 on the Sn90-In10 wt% alloy wire instead of creating a textured surface around the periphery of the glass surface. The design process for sample 'A4' has two stages implemented for construction, as illustrated schematically in Fig. 9a. The first stage was to produce the textured surface on the Sn90-In10 wt% alloy wire to be placed around the periphery of the lower glass sheet and lower the top glass sheet on to the bottom sheet. The second stage was to place the two glass sheets together, separated by the support pillars inside the oven and then use the heating regime followed by evacuation and pump-out hole sealing.

The detailed construction process implemented for sample 'A4' is as follows:

(i) Two Pilkington k-glass sheets were sliced to the size of 170mm·170·4mm. A pump-out hole (4mm in diameter) was drilled in a sheet of upper glass for evacuation located at 75 mm from two corner edges. The glass sheets were cleaned with water, isopropanol and acetone followed by initial bake-out in an oven at 120˚C.

(ii) A Sn90-In10 wt% alloy wire was shaped to the sealing area and covered in B_2O_3 inside the oven which was then heated up to 250˚C shown in Fig. 5.29. The wire with a coating of B_2O_3 was placed around the periphery of the lower glass sheet.

(iii) Stainless steel support pillars were positioned on the lower glass sheets in a square array of pitch 24mm. The upper glass sheet was lowered on to the support pillars.

(iv) The sample was heated in an oven to 450˚C following the heating regime shown in Fig. 4.

(v) The evacuation of the sample 'A4' was performed by placing it on a hot plate and heated to maximum of 150˚C and the use of high-vacuum pump out system as similar to sample 'A3'.

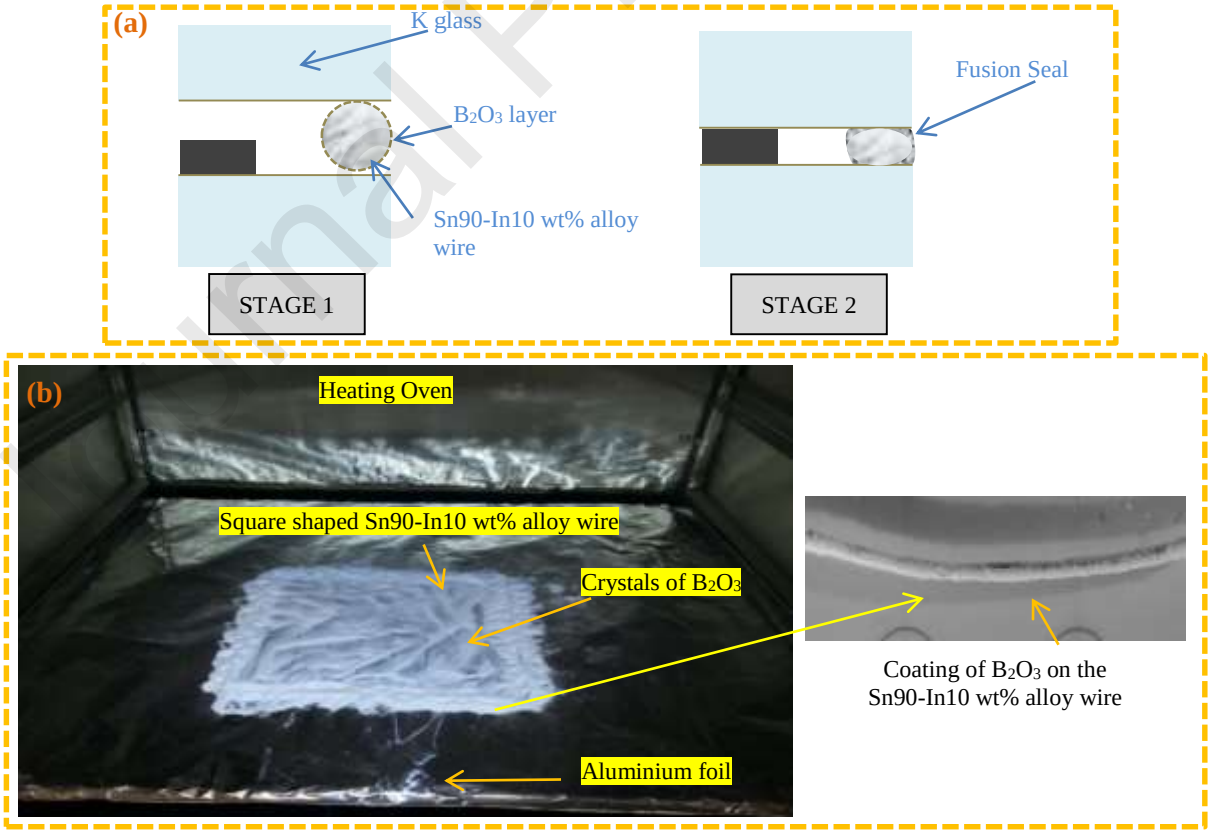

Fig. 9. Illustrates (a) two stage profess for sample 'A4' in which (b) the formation of a B_2O_3 textured layer on the Sn90-In10 wt% alloy wire to be placed around the periphery of the glass sheet followed by heat the complete sample to 450˚C to form the seal.

After more than 20 experimental trials, a viable design and construction process was achieved and the preceding experiments are just a few that helped to achieve this novel process for the successful construction of fusion edge-sealed vacuum glazing (sample 'A5') area of 300mm·300mm. The sample 'A5' is a Pb-free, ultrasonic-soldering free and low-cost edge sealing solution. This method reduces the time required for vacuum glazing construction. The sample 'A5' is a modified design based on sample 'A3' discussed in section 4.3. The textured surface on the glass was based on sample 'CF', discussed in section 3. The design process for fusion edge-sealed vacuum glazing, sample 'A5', has three stages implemented for construction, as illustrated schematically in Fig. 10a. The first stage was to produce a fine powder of crystalline B_2O_3 (≈ 74 microns) of B_2O_3 crystals to be mixed with Sn powder (grain size smaller than 44 micron) having the proportions of ratio 38:62 by wt%, respectively, ($B_2O_3$38-Sn62 wt% mixture). This was then used to texture a surface around the periphery of the two glass sheets. The Second stage was to prepare and place two Sn90-In10 wt% alloy wires in a rectangular arrangement on the textured area on the bottom sheet. The third stage was to place the two glass sheets together, separated by the support pillars inside the oven and then use the heating regime in Fig. 4.

The detailed construction process implemented for sample 'A5', which is the successful construction of fusion edge-sealed vacuum glazing, is as follows:

(i) Two Pilkington k-glass sheets were sliced to the size of 300·300 mm. A pump-out hole (4mm in diameter) was drilled in a sheet of upper glass for evacuation located at 75 mm from two corner edges. The glass sheets were cleaned with water, isopropanol and acetone followed by initial bake-out in an oven at 120˚C.

(ii) A mixture of $B_2O_3$38-Sn62 wt% was prepared to form surface texture around the periphery (12mm width) of the two glass sheets. This was achieved by heating to 450˚C following the heating regime shown in the Fig. 4.

(iii) A Sn90-In10 wt% alloy wire (2mm in diameter) was positioned on the textured edge sealing area of the lower glass sheet.

(iv) Stainless steel support pillars were positioned on the lower glass sheets in a square array of pitch 24mm. The upper glass sheet was lowered on to the support pillars.

(v) The whole sample 'A5' was heated in an oven to 450˚C following the heating regime shown in Fig. 4 to join the two glass sheets.

(vi) The sample 'A5' was evacuated by placing it on a hot plate and heated to a maximum temperature of 50±5 ˚C. This process of low-temperature surface induction on evacuation is achieved after rigorous experiments detailed in Memon *et al* (2018) for better evacuation and pump-out hole sealing, the evacuation and heating arrangement is shown in Fig. 10b.

(vii) During evacuation the pump-out hole was successfully sealed with a glass square (which was ultrasonically solder coated with Cerasolzer CS-186 alloy) using the cartridge heater mounted inside the vacuum cup. It is pertinent to mention here that the pump-out sealing with glass square approach can be avoided if constructed inside the vacuum chamber. Thus, the pump-out hole was sealed with CS-186 is a temporary laboratory-based solution.

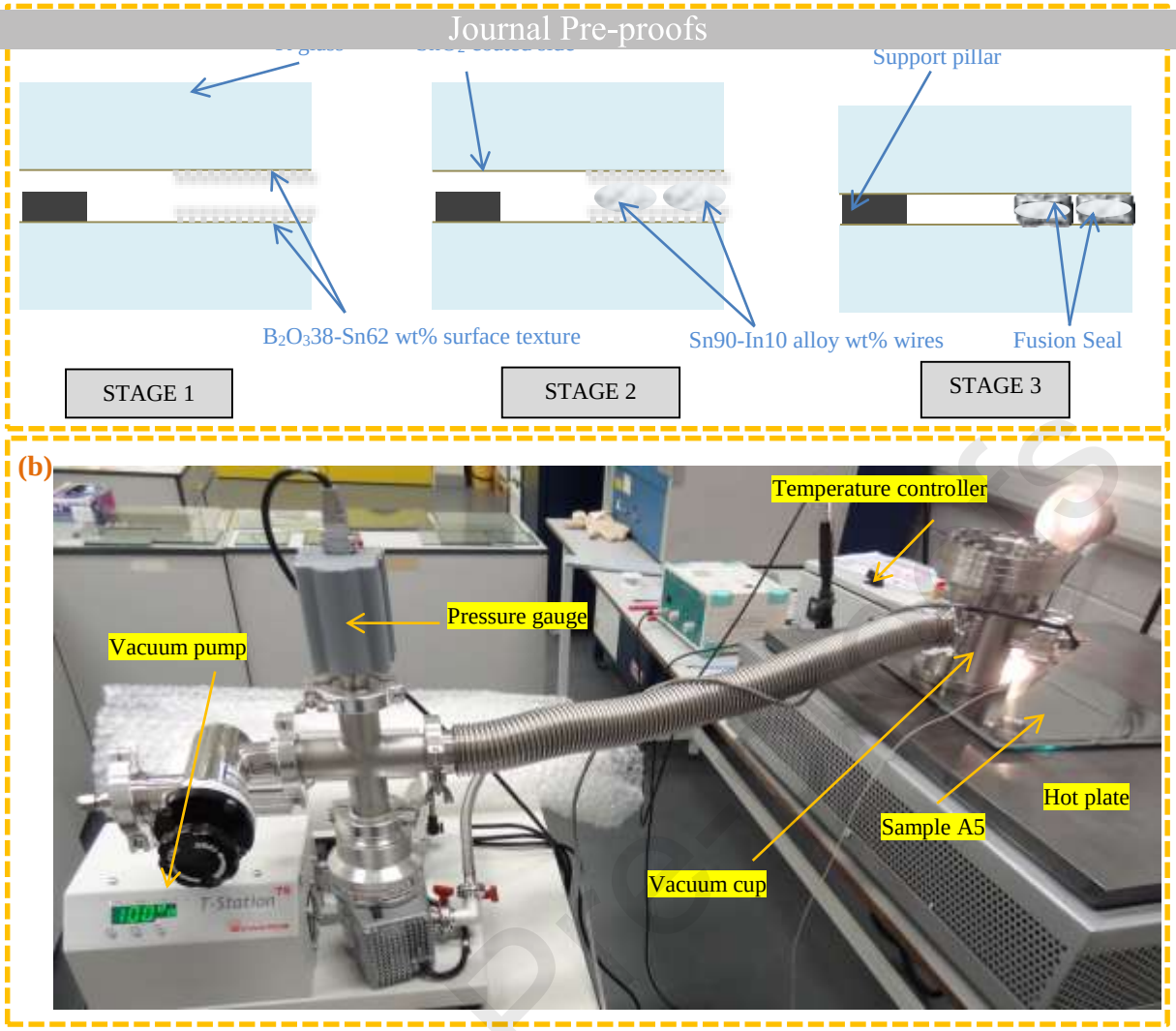

Fig. 10. (a) The three-stage design process implemented for the construction of sample 'A5' (fusion edge-sealed vacuum glazing), and (b) experimental setup for the evacuation of sample 'A5' with low-temperature surface heat induction to 50±5 ˚C for better evacuation and pump-out hole seal.

5. Experimental results and discussions

From the experiments undertaken and experience developed for 9 years, the Sn metal wettability and stability on the surface of glass are observed to be very complicated. If fabricating a vacuum glass sample using Sn metal on its own, then the issues of seal reliability and the long-term stability of the vacuum arises. Even the use of metal alloys such as In-Sn and/or Bi-Sn could not make a rigid air-tight seal between the two sheets of glass on itself. In this particular research work, one of the objectives was to investigate the application of cost-effective metals such as Sn and other Pb-free high-temperature edge sealing materials for the formation of a hermetic glass edge seal for vacuum glazing. The second objective of this research was to investigate methods and techniques that could make ultrasonic soldering unnecessary for edge seal formation. This, eventually, will provide savings in manufacturing time, electricity and material quantities/costs. In comparing to previous work (by the group at the University of Ulster) where external pressure was required to form a pure In seal, in these methods there was no need to apply an external pressure as the weight of the glass sheet was enough to press the Sn90-In10 wt% alloy wire onto the $B_2O_3$38-Sn62 wt% rigid glass-metallic surface texture during heating regime.

At least 60 samples were constructed using different techniques and Pb-free materials such as B_2O_3, Sn, Bi and/or Zn in combination with pure Sn solder wire or Sn90-In10 wt% alloy. In this paper, only five vacuum glazing samples are discussed in detail. In which, 20 trials were for the sample A5 and it is the most successful in achieving a hermetic fusion edge-seal. This sample was evacuated and sealed; the stress patterns were clearly visible after pump-out sealing. In the following sub-sections, the results of the performance of samples 'A1', 'A2', 'A3', 'A4' and 'A5' are experimentally analysed.

5.1. Sample 'A1'

The bond formation in sample 'A1' was based on a reaction between the B_2O_3 layer and the solid Sn soldered layer. This was believed (at that time) to produce an air-tight glass edge seal. The known challenge of matching the thermal expansion of Sn with the glass surface has already been discussed earlier in section 1 and 3. The behaviour of the B_2O_3 crystals changes when heated in an oven. It was found that the temperature control and the heating environment influenced the quality of fusion edge-seal. It can be seen from Fig. 11a that sample 'A1' is mostly oxidised in the 14mm wide edge area shown by colour change to a slightly blackened colour in some areas of the edge. Despite the limitations/weaknesses in sample 'A1', the sample was placed in the oven at 80˚C and evacuated whilst in the oven. Sample 'A1' achieved a vacuum pressure of 0.1 Pa during evacuation at 80˚C. Stress patterns across the pillars were observed during evacuation. After evacuation the level of vacuum pressure was initially maintained at 10 Pa and then increased to 100 Pa but not to atmospheric pressure (1.31kPa). This sample was re-evacuated three times and displayed similar evacuation performance, as illustrated in the Fig 11b. This gave confidence that by improving this method a sample could achieve better evacuation pressure. At this stage, sample 'A1' was considered not sealed due to the insufficient level of vacuum pressure readings and the pump-out hole was not sealed.

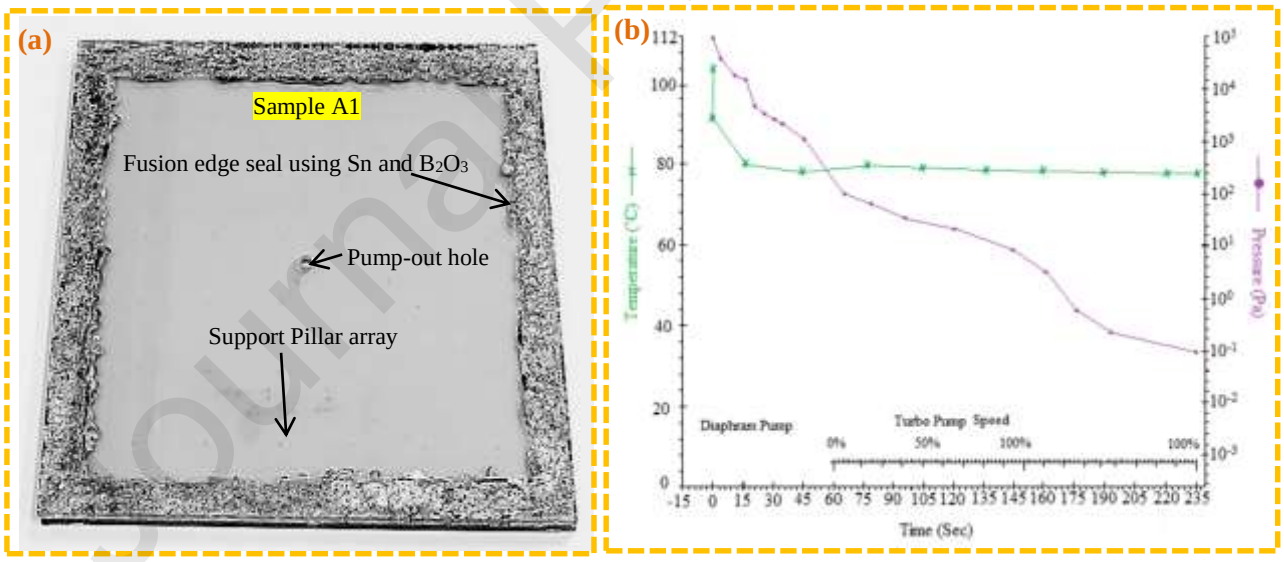

Fig. 11. Experimental results show (a) sample 'A1' constructed with B_2O_3 texture layer and ultrasonically soldered Sn wire on the edges of the two glass sheets and (b) hot-plate surface temperature induction and vacuum pressure measurements showing evacuation and heating of sample 'A1'.

The sample 'A2' was constructed using Sn90-In10 wt% alloy instead of Sn wire with similar techniques and evacuation process as used in sample 'A1'. Stress patterns were observed during evacuation and the pump-out hole was sealed with Cerasolzer-CS186 alloy as shown in Fig. 12a. Sample 'A2' pump-out vacuum pressure was lower than for sample 'A1' with a value of 0.095Pa achieved at the hot-plate surface temperature of 80˚C. Typical hot-plate surface temperature induction and vacuum pressure profiles for evacuation and pump-out hole sealing are shown in Fig. 12b. This sample 'A2' gave a positive indication that the surface texture and the use of Sn90-In10 wt% alloy can be improved. It was found that the soldering difficulties are less when compared to pure Sn. The practice of ultrasonic soldering was considered to be complicated due to the risk of oxidation and pin-hole formation during soldering on the textured surface.

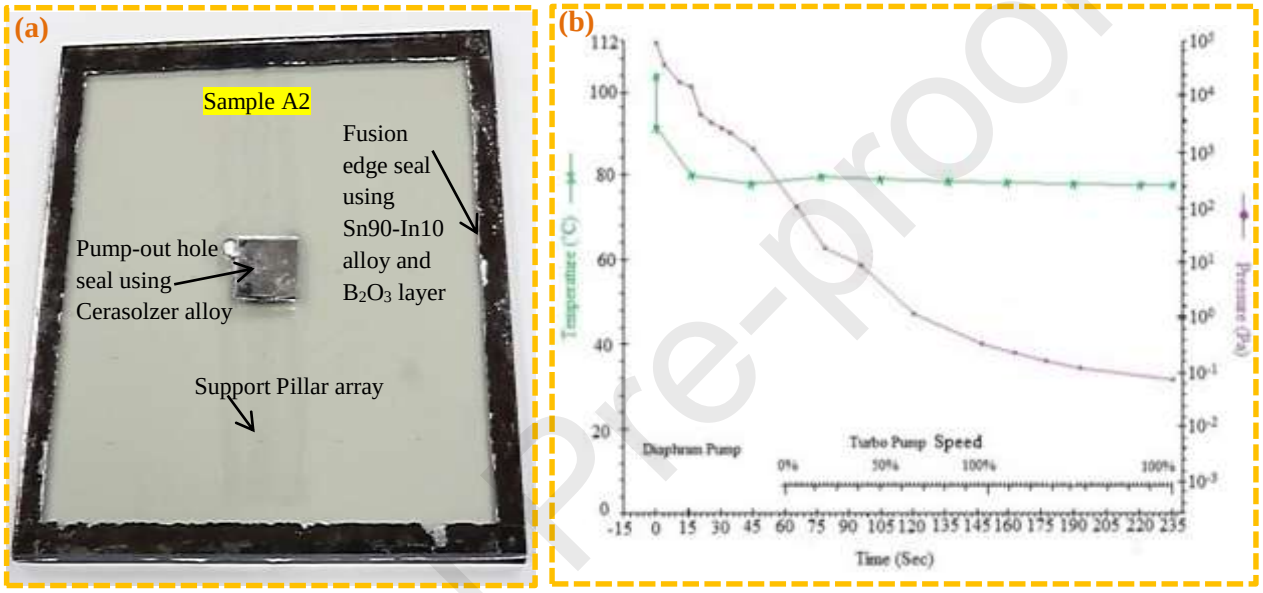

Fig. 12. Experimental results show (a) sample 'A2' constructed with B_2O_3 texture layer and ultrasonically soldered Sn90-In10 wt% alloy on the edges of the two glass sheets and (b) hot-plate surface temperature induction and vacuum pressure measurements showing evacuation and heating of sample 'A2'.

5.3. Sample 'A3'

The sample 'A3' was based on the improved techniques and method of making the glass edge seal discussed in section 4.3. The soldering process gave an increased risk of leaving traces of oxides in the seal. The sample A3, as shown in Fig. 13a, was constructed based on a simple ultrasonic-soldering free technique. The seal was formed from two B_2O_3 textured layers on Sn90-In10 wt% alloy solder wire. The pump-out hole was sealed using Cerasolzer-CS186 alloy. This technique was considered an effective method for producing a small size (such as 150mm·150 mm). The stress patterns were observed during evacuation. The vacuum pressure in the sample 'A3' was achieved to be 0.1 Pa whilst the hot-plate surface temperature induction increased to 150˚C, to understand the influence of higher temperature on evacuation improvements whilst keeping below the thermal shock or saturation/break point. Typical hot-plate surface temperature induction and vacuum pressure profiles for evacuation and heating are shown in Fig. 13b. This sample provided positive indication that using a Sn90-In10 wt% alloy without ultrasonic soldering could form an effective hermetic fusion edge seal. However, in this sample the correct vacuum pressure was not achieved due to the level of outgassing. It was observed that the crystals of B_2O_3 and Sn90-In10 wt% alloy

were incompatible. This technique was repeated with the modification of making a thin textured layer of B_2O_3 on the Sn90-In10 wt% alloy in sample 'A4'.

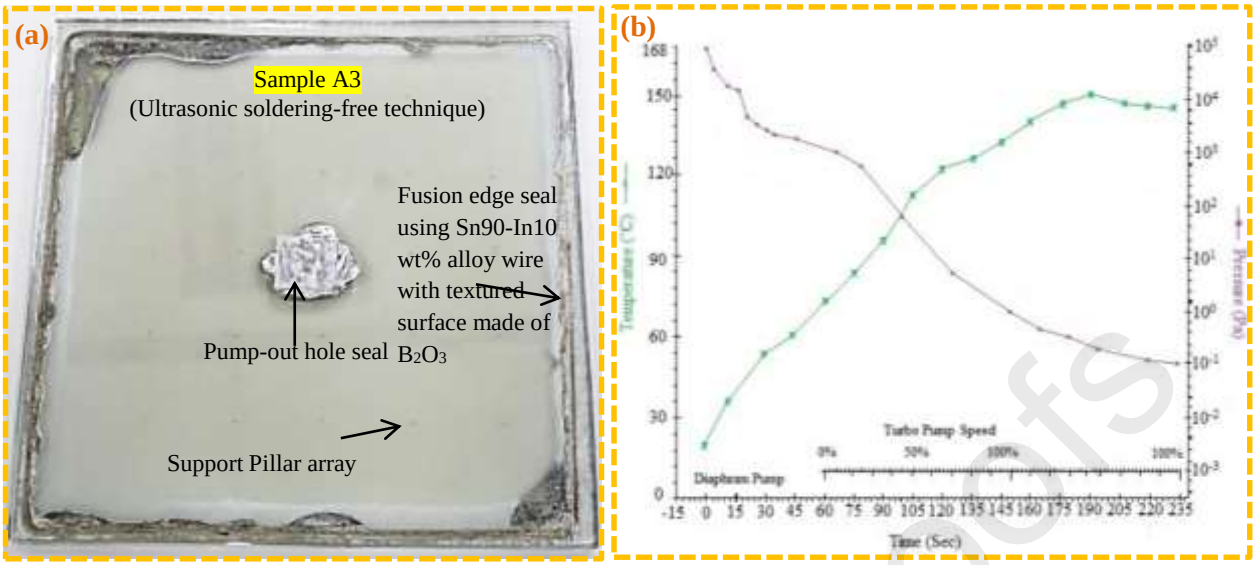

Fig. 13. Experimental results show (a) sample 'A3' constructed with a B_2O_3 texture layer and Sn90-In10 wt% alloy wire positioned on the edges of the two glass sheets without using ultrasonic soldering, and (b) hot-plate surface temperature induction and vacuum pressure measurements showing evacuation and heating of sample 'A3'.

5.4. Sample 'A4'

The sample 'A4', shown in Fig. 14a, achieved a vacuum pressure down to 0.1 Pa during evacuation. It was observed that glass bending and expansion occurred due to the pressure difference of vacuum cavity and the atmosphere and the temperature distribution due to the hot-plate surface temperature being increased to 150˚C. The edge seal area of sample 'A4' cracked and the vacuum pressure was lost. Thus, this sample did not go through the pump-out hole sealing stage. It is pertinent to mention that vacuum glazing is sensitive because it has to experience increasing level of internal compressive and external tensile stresses and the edge-seal must be able to withstand such shear forces. The hot-plate surface temperature induction and pressure profiles for evacuation and heating of sample 'A4' are shown in Fig 14b. It was resulted from this sample 'A4' that the hot-plate surface temperature has to be reduced in order to minimise additional stresses during evacuation and pump-out hole sealing. The microstructural investigations discussed in section 3 showed that the appropriate mixture of B_2O_3 and Sn powders produces rigid glass-metallic interaction with Sn90In10 wt% alloy. A series of further constructions were made that helped to modify the construction approach and results for sample 'A5' are discussed in section 5.5.

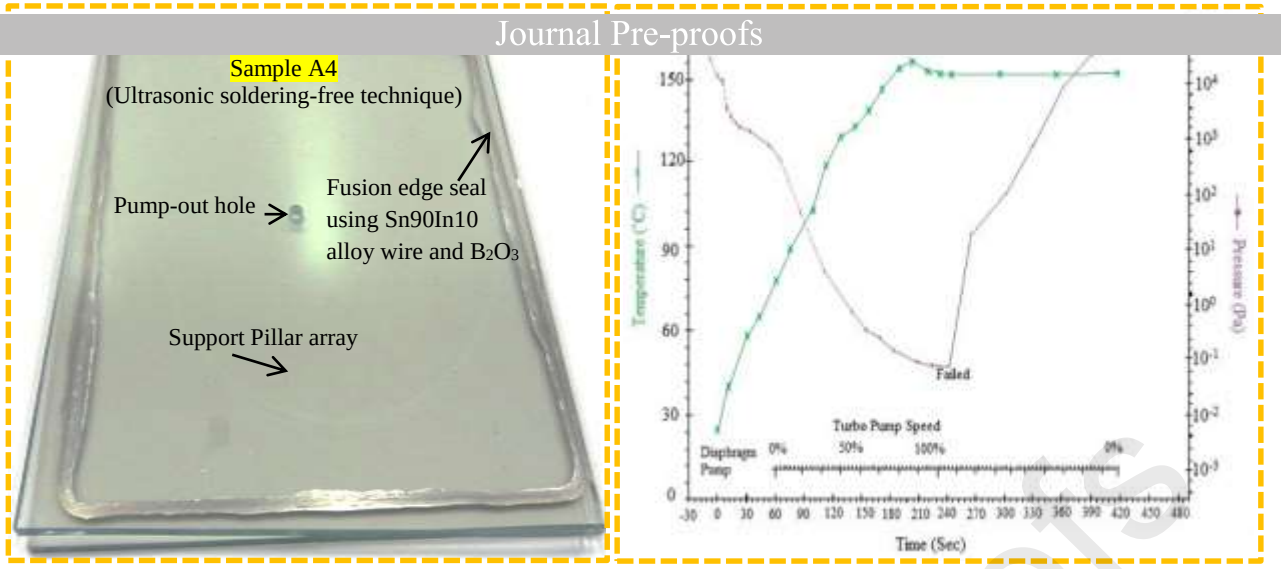

Fig. 14. Experimental results show (a) sample 'A4' constructed with a thin textured layer of B_2O_3 on the Sn90-In10 wt% alloy wire positioned between the glass sheets and heated without using the ultrasonic soldering method, and (b) typical temperature/pressure profiles for evacuation and heating of sample 'A4'.

5.5. Sample A5 (fusion edge-sealed vacuum glazing)

The preceding experiments, designs and seal analysis provided confidence in achieving a hermetic glass edge seal around the periphery of glass sheets with a lead-free and ultrasonic-soldering free approach. The sample 'A5' successfully constructed and is the basis of at least 60 samples, among which five are discussed in this paper. The fusion edge seal of sample 'A5' is based on the Sn90-In10 wt% alloy and the $B_2O_3$38-Sn62 wt% bonded glass-metalled textured surface as shown in Fig. 15a. This sample was comparatively simple to design and required less time for construction compared to other techniques where metal alloys are soldered around the edges of the glass surface. The technique was also modified based on preceding sample constructions. The sample 'A5' was heated during evacuation to not more than 50±5 ˚C for better evacuation and pump-out hole seal. Soldering was not used other than for pump-out glass square cover slip. The pump-out hole of sample 'A5', as shown in Fig. 15a, was successfully sealed with Cerasolzer-CS186 alloy after 6-7 hours of evacuation. The reason to evacuate longer is to avoid adsorbed gaseous molecules as a thin layer on the internal surfaces within the tubes and cavity of fusion edge-sealed vacuum glazing. The experimental examination shows repetitive behaviour of stress patterns, during evacuation and after pump-out hole seal, across the support pillars indicated a hermetic (vacuum-tight) edge seal. This sample achieved a vacuum pressure of $8.2 \cdot 10^{-4}$ Pa when the hot plate surface temperature induction was maintained at 50±5˚C to reduce stresses due to temperature gradients. These experimental results also validate the temperature induced stresses, and subsequent stresses observed are tensile on top sheet of glass and higher compressive on bottom sheet of glass, analysed elsewhere [44-48]. 20 trials of similar sample ('A5') having different sizes constructed verifies the persistent fusion edge-seal at the accuracy of 99.5% of cavity vacuum pressure. One of the important issues in fusion edge-sealed vacuum glazing is its long-term stability of vacuum pressure. It was found after four months of observation the sample 'A5' resembles the similar stress patterns across support pillars. Typical hot-plate surface temperature induction and vacuum pressure profiles for evacuation and heating are shown in Fig. 15b. To microstructurally analyse the seal, the sealing area of a separate smaller sample was deliberately fractured and the surface texture was found as thin glass-metallic layer of $B_2O_3$38-Sn62 wt% on the Sn90-In10 wt% alloy, shown in Fig. 15a.

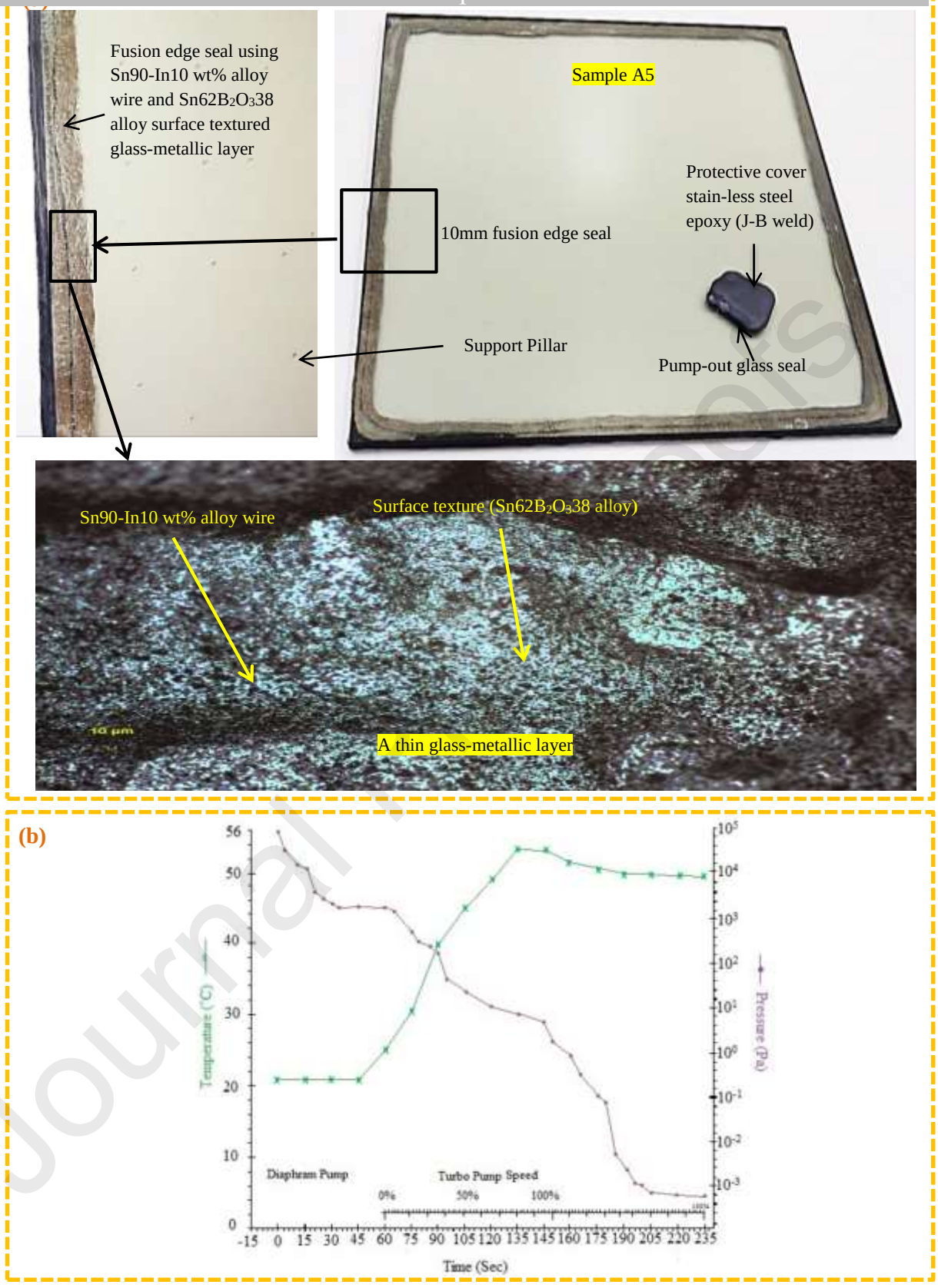

Fig. 15. Experimental results show (a) sample 'A5' fusion edge-sealed vacuum glazing constructed with a thin glass-metallic textured layer (B_2O_338- Sn62 wt% mixture) on the Sn90-In10 wt% alloy, and (b) hot-plate surface temperature induction versus vacuum pressure measurements profiles showing evacuation and heating of sample 'A5'.

6.1. Validated finite element modelling approach

A validated three-dimensional finite element model (FEM) of Memon et al (2015) [19] was employed for the thermal performance analysis of constructed fusion edge-sealed vacuum glazing, area of 300mm·300mm with 10 mm wide fusion edge seal. The details of the analytical model approach is reported elsewhere by Memon et al. (2019) [12] and Fang et al. (2006) [49] in which a validated set of equations, including direct representation of the support pillars utilised in the FEM were solved for the constructed design of sample 'A5' (fusion edge-sealed vacuum glazing) at the cavity vacuum pressure of $8.2 \cdot 10^{-4}$ Pa. Due to symmetry conditions, and to reduce the computational effort required, only one quarter (150mm·150mm) of the sample 'A5' was simulated. The model was implemented using eight node iso-parametric elements (type 43 in MSC Marc) using a total of 94036 elements and 113012 nodes to model one quarter of the fusion edge-sealed vacuum glazing as shown in Fig. 16. A vacuum cavity of 0.15 mm high was modelled with a thermal conductivity considered near to zero, knowing at $8.2 \cdot 10^{-4}$ Pa the mean-free path between gaseous molecules will be higher than 300 m, thus the heat transfers through conduction and convection in the cavity are infinitesimal. However, heat transfer by long-wave radiation between the two internal glass surfaces coated with low-emissivity SnO_2 coatings was incorporated by employing a 6 μm layer on the inner surface of the glass sheet with the emissivity of SnO_2. The cylindrical pillars of radius *r* implemented in this model represented by the same number of pillars with the same cross-sectional areas in the developed finite-element model. For simplicity, the cylindrical pillars were approximated by a square cross-section in the model with side length 1.78*r*, as both pillar shapes with the same cross-sectional area will conduct similar amounts of heat under the same boundary conditions [19, 47]. A graded mesh with a higher number of elements in the pillars was employed to achieve adequate representation of the heat transfer and the accuracy is in good agreement with [19, 50]. A string of convergence simulation tests was performed to ensure that the density of the elements used was sufficient to predict the thermal performance with an accuracy of more than 95%. The material properties and parameters of the simulated fusion edge-sealed vacuum glazing (sample 'A5') are listed in Table 2. For the simulations, the indoor warm–side and outdoor cold-side internal and external surface air temperatures were set to be at 21.1˚C and -17.8˚C respectively in line with ASTM specified test conditions for glazings in winter conditions [51]. The internal and external surface heat transfer coefficients were set to 8.3 $Wm^{-2}K^{-1}$ and 30 $Wm^{-2}K^{-1}$ respectively [19, 52]. The glass surface to surface thermal transmittance of the centre-of-pane and total glazing were calculated from equations reported in Memon et al. (2015) [19] and Memon et al. (2018) [53].

Table 2
Parameters and material properties of the components employed in the finite element modelling for fusion edge-sealed vacuum glazing.

Parameter	Description	Value/Type
Vacuum Glazing dimensions	Top glass sheet	300·300·4mm
	Bottom glass sheet	300·300·4mm
Glass sheet	Thermal conductivity	1 $Wm^{-1}K^{-1}$ [53]
Emittance	Two surfaces (Hard coating)	0.15/SnO_2
Fusion edge seal	Material	Sn90-In10 wt% alloy
	Width	10mm
	Thermal conductivity	62.8 $Wm^{-1}K^{-1}$
Thin glass-metallic layer	$B_2O_3$38- Sn62 wt% mixture	0.937$Wm^{-1}K^{-1}$
Support Pillar	Material	Stainless steel 304
	Diameter	0.3mm
	Height	0.15mm
	Pillar separation	24mm
	Thermal Conductivity	16.2$Wm^{-1}K^{-1}$ [19]

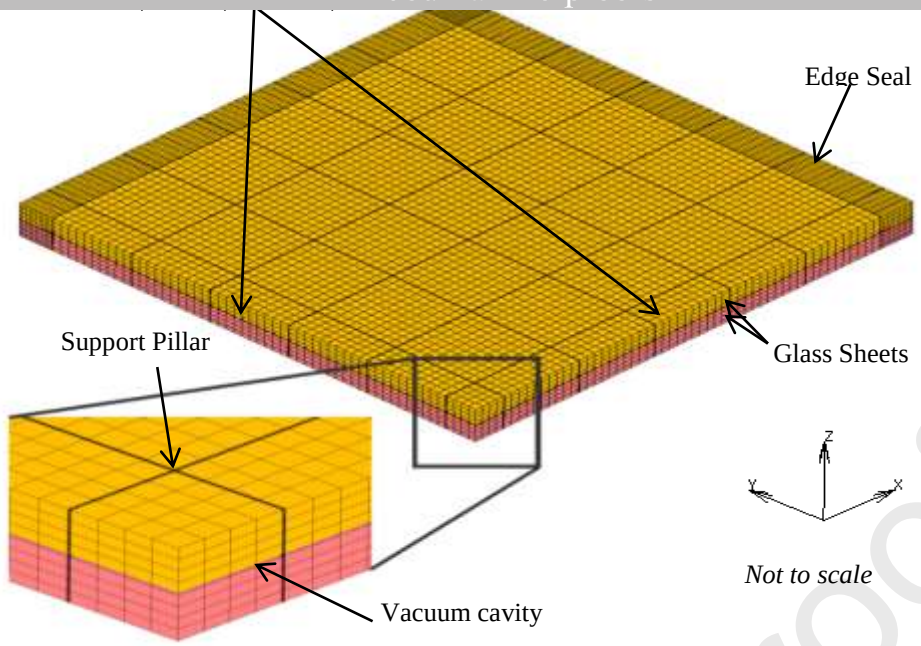

Fig. 16. Finite element mesh of the quarter (150mm·150mm) of the fusion edge-sealed vacuum glazing.

6.2. Thermal performance analysis

The thermal analysis of fusion edge-sealed vacuum glazing, area of 300mm·300mm with 10 mm wide fusion edge seal, was performed and achieved the centre-of-sheet thermal transmittance value (U_c value) of 1.039 $Wm^{-2}K^{-1}$ and total thermal transmittance value (U_t value) of 1.039 $Wm^{-2}K^{-1}$.When compared to Zhao *et al* (2007) [54] predictions, the U_c value and U_t value with frame were reported to be 1 $Wm^{-2}K^{-1}$ and 1.19 $Wm^{-2}K^{-1}$, respectively. These reported values were based on an indium edge-sealed vacuum glazing, area of 400mm·400mm with 6 mm wide seal and SnO_2 coatings on the inner surface of two glass sheets with a pillar spacing of 25mm. An increase of 0.039 $Wm^{-2}K^{-1}$ and 0.21 $Wm^{-2}K^{-1}$ in the U_c and U_t values, of the fusion edge-sealed vacuum glazing, was due to the use of a 10mm wide edge seal, closer pillar spacing of 24mm, and the smaller size of this sample. The wider layer of edge seal causes increased edge effects which results in higher U values of the vacuum glazing. The total heat transfer can be further be minimised by reducing the width of edge seal to 6mm. For example, a 6mm wide indium edge-sealed vacuum glazing was predicted to have U_t and U_c value of 0.9 $Wm^{-2}K^{-1}$ and 0.36 $Wm^{-2}K^{-1}$, respectively, using soft low emittance (Ag) coatings [18]. The thermal conductance values (centre-of-sheet and total) of the fusion edge-sealed vacuum glazing were predicted to be 1.24 $Wm^{-2}K^{-1}$ and 1.79 $Wm^{-2}K^{-1}$, respectively. Collins and Simko (1998) [11] predicted the centre-of-sheet thermal conductance from 3 $Wm^{-2}K^{-1}$ (for vacuum glazing with no internal low emittance coating) to 0.8 $Wm^{-2}K^{-1}$ (for vacuum glazing with the two SnO_2 internal low emittance coatings) for area of 1m·1m of vacuum glazing with an approximate 10mm solder glass edge seal. Comparing it with the fusion edge-sealed vacuum glazing, an increase in U_c value of 0.44 $Wm^{-2}.K^{-1}$ occurred due to its smaller size (300mm·300mm).

The heat transfer modelled includes the heat flux from the indoor (warm) side to the indoor glazing surface. Heat transfer by long wave radiation between the two inner glass surfaces within the vacuum gap. Heat transfer by conduction through the support pillars, the10mm wide layer of the edge seal and the glass. Heat flux from the outdoor (cold) surface of the glass to outdoor ambient air. Isotherms of the cold and warm side of the fusion edge-sealed vacuum glazing are presented in Fig. 17, Fig. 18 and Fig. 19.

The mean glass surface temperature resulted was of 7.03˚C and -13.47˚C on the cold and warm sides of the total glazing area, respectively. The temperature variation due to heat conduction through the support pillars on the central glazing area was predicted to be 0.65˚C and 0.68˚C on the cold and hot sides of the glazing surfaces, as shown in Fig. 17. It can be seen that the temperature variations in the central glazing area on the cold side between the support pillar and the vacuum layer is smaller than on the warm side. The predictions made by Fang *et al* (2009) [52] gave temperature variations of 0.35˚C and 0.37˚C through the support pillars in the central glazing area. Differences in predictions of heat transfer through the vacuum glazing were caused by a number of reasons such as: the use of a 10mm wide layer of an edge seal; the smaller, 300·300mm, glazed area; and different thermal properties used for k-glass and stainless steel type 304 pillar whose thermal properties were obtained from the manufacturer's datasheets.

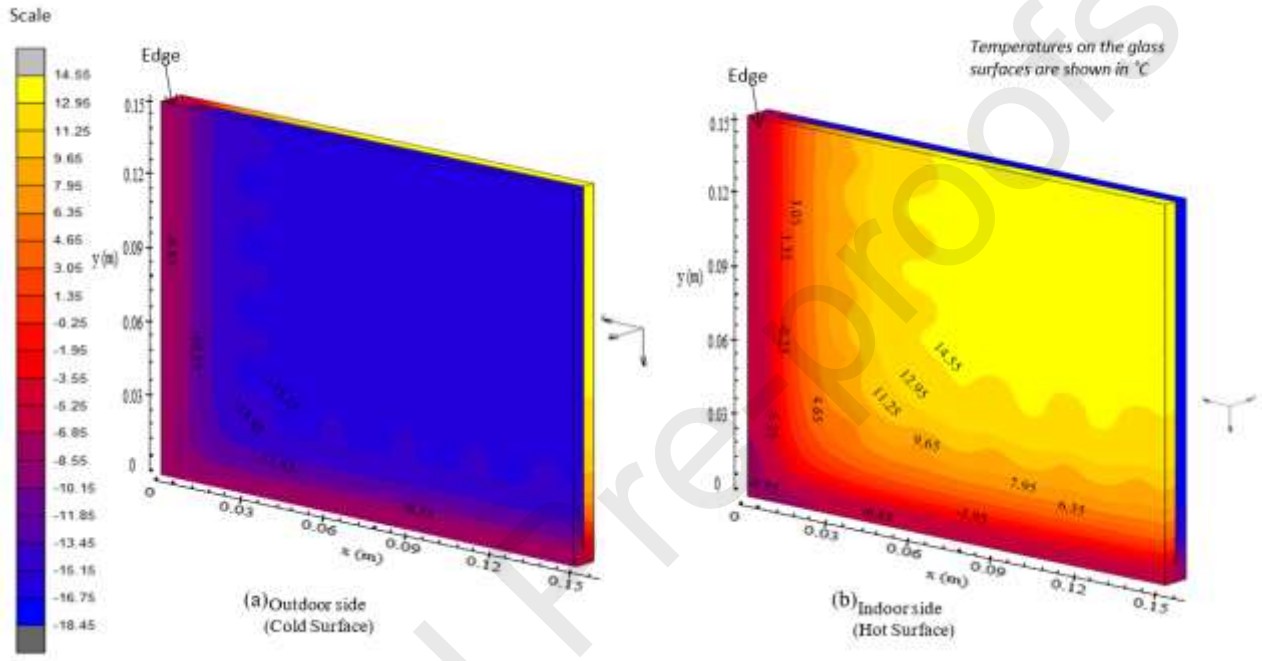

Fig. 17. Predicted isotherms on (a) the cold (outdoor) surface showing an increase of temperature from the centre area to the edge area, and (b) the warm (indoor) surface showing a decrease of temperature from the centre area to the edge area of the simulated fusion edge-sealed vacuum glazing using ASTM boundary conditions.

Fig. 18 and Fig. 19 show the greater influence of edge effects due to the use of a 10mm wide seal, the edge effects can be seen up to a distance of 72mm and 45mm from the edge on the warm and cold side surface of the vacuum glazing, respectively. The overall fusion edge-sealed vacuum glazing thermal performance can be improved by reducing the width of edge seal to 6mm. However, the fusion edge-sealed vacuum glazing is based on a high temperature (450˚C) construction process, so there are restrictions in the use of soft-low emittance coatings, e.g. silver coatings, and tempered glass.

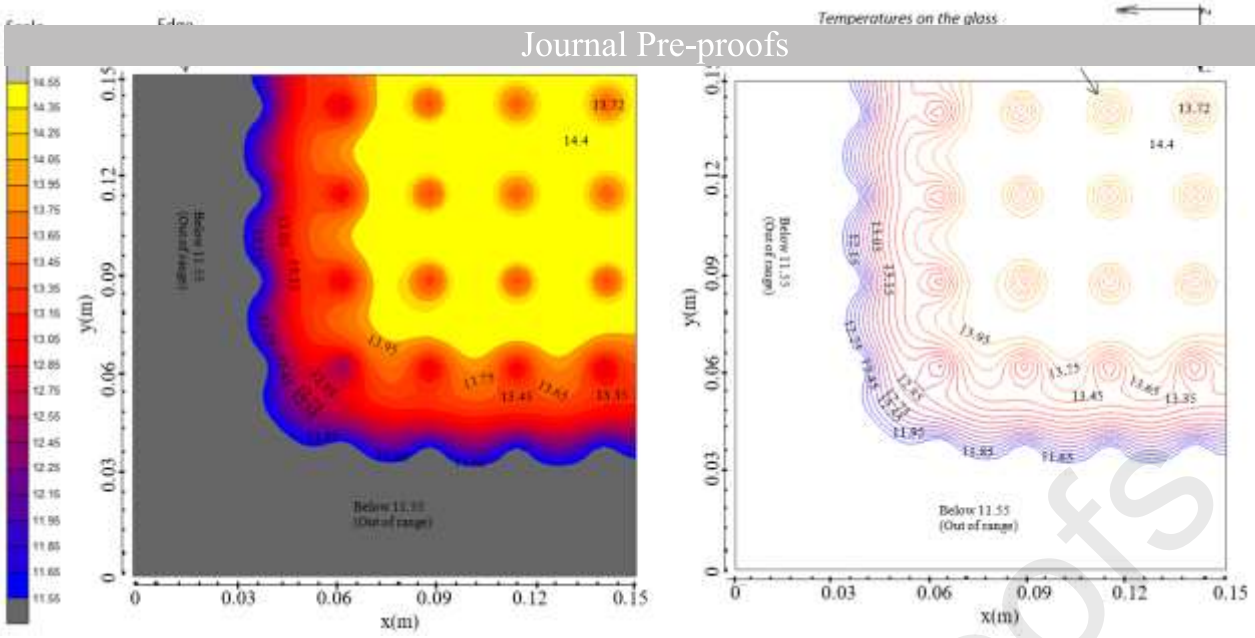

Fig. 18. Predicted isotherms on the warm (indoor) side of the glass surface over a refined temperature to the temperature variations around the support pillars in the central area of the simulated fusion edge-sealed vacuum glazing.

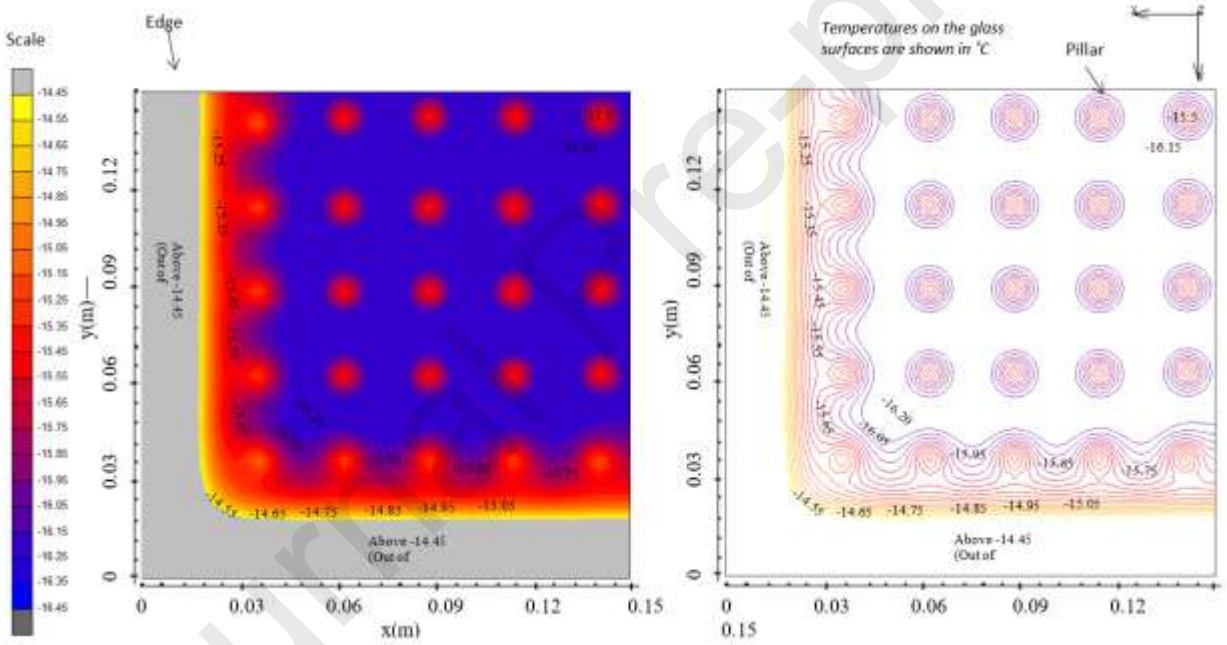

Fig. 19. Predicted isotherms on the cold(outdoor) glass surface over a refined temperature range to show the temperature variations around the support pillars in the central area of the simulated fusion edge-sealed vacuum glazing.

7. Comparative cost analysis of edge sealing materials

Cost is a significant challenge, and complex issue, that determines the realistic implications of vacuum glazing construction at mass manufacturing level. It is appropriate to mention that the cost analysis presented here is for the edge sealing materials only and the cost analysis is based on the cost at the laboratory level. The edge sealing materials cost is dependent on the supplying company's location, quantity required and purity of products supplied. A further important factor to consider is the wide variation in market prices of materials. At the mass manufacturing level, the cost of the materials will be reduced significantly and will depend on the metal stock exchange rate. It was not possible to get price

quotes at larger quantity of materials for mass production as the designed fusion sealing materials are new. The fusion edge seal materials consumed for the construction of vacuum glazing were compared with solder glass edge sealing materials. The solder glass materials are available from the Schott glass company. The solder glass based sample costs based are on the assumption that the quantity required for sealing would be similar to the fusion sealing method. This assumption was based on experiments with samples using powdered metals. Two types of solder glasses were analysed both containing a percentage of lead, as described in the Table 5.3. The cost of solder glass sealing contributes a small part to the cost of vacuum glazing. Furthermore, with the two low-e glass sheets the cost of the vacuum glazing was reported to be US $40±7 per m^2 at the manufacturing level in 1995 [55]. To date, solder glass sealed vacuum glazings are fabricated in Japan by Nippon Sheet Glass Company under a trade name of SPACIA [56]. The cost per m^2 in US $150 is dependent on the size/shape and quantity of the product [57]. It must be noted that the net profit margin in the prices of materials by supplying companies is not considered.

Table 3
The measured and predicted costs of the glass edge sealing materials used for the construction of vacuum glazing units.

Sample	**Area (mm)**	**Materials quantity (grams)**								**Total cost in GBP**	**Cost in GBP per m^2**
		Sn	B_2O_3	Sn metal wire	Sn90In10 alloy wire	Solder glass G017-052	Solder glass 8467	Pump-out hole Seal			
								Cerasolzer alloy CS186	J-B Weld		
'A1'	150·150	-	0.73	13.88	-	-	-	-	-	4.9	32.67
'A2'	150·150	-	1.16	-	21.95	-	-	0.6	0.22	2.19	11.48
'A3'	150·150	-	0.727	-	13.81	-	-	0.6	0.22	1.58	7.42
'A4'	170·170	-	0.824	-	15.66	-	-	0.6	0.22	1.72	7.42
'A5'	300·300	1.22	0.75	-	37.26	-	-	0.85	0.42	3.72	10.56 (Whole glazing= 38.45)
'A6'*	300·300	-	-	-	-	40	-	0.85	0.42	16.02	54.19
'A7'*	300·300	-	-	-	-	-	40	0.85	0.42	27.80	90.83

* These samples were not fabricated in the laboratory, here predicting the amount of material consumed based on the fabricated samples.

The measured and predicted costs for the edge sealing materials utilised are presented in Table. 3. The cost of sample 'A1' was calculated to be GBP 4.90 for the 150mm·50mm sample, this cost was partly due to the small quantity purchased from the supplier (Advent-rm) [43]. The cost of sealing materials, including the pump-out hole sealing, utilised in sample 'A2' (area of 150mm·150mm), 'A3' (area of 150mm·150mm) and 'A4' (area of 170mm·170mm) was GBP 2.19, GBP 1.58 and GBP 1.72, respectively. The cost of sample 'A5' (area of 300mm·300mm) was calculated to be GBP 3.72 and GBP 10.56 per m^2; pump-out hole sealing was included. The quantity of the solder glass sealing material predicted to be used was 40 grams. Comparing to the predicted solder glass based sample 'A6' and 'A7', the fusion edge-sealed vacuum glazing reduces the cost to 75.8% (GBP 43.63) and 86.84% (GBP 80.27), respectively. This was based on the 10mm width of the edge seal and the quantity used/consumed, as discussed by Collins and Robinson (1998). It is well known that laboratory-based costs of sample construction are generally much higher than the cost at the manufacturing level. However, the fusion edge-sealed vacuum glazing under these conditions is seemed to be the most low-cost solution for mass production.

8. Conclusions

Advancement in hermetic (vacuum-tight) edge-sealing materials has been one of the challenges since decades because of the existing cost, durability, use of hazardous substance and complexity-to-construct issues in vacuum glazing's that this paper presented novel experimental findings with designs and methods developed to construct and analyse thermal performance of the fusion edge-sealed vacuum glazing. The fusion edge-seal is a cost-effective, energy efficient (ultrasonic soldering free), and Pd-free (hazardous substance free) solution, it has a potential for mass production. The main conclusions are summarised into the following four characteristics:

- The novel concept of forming a thin glass-metallic textured layer on the surface of a glass sheet is achieved. This was the result of the creation of interaction between glass and metal with rigid bonded surface texture, in which the formation processes and experimental glass-metallic textured surface bonding property tests of 15 samples are microstructurally analysed using FIB-SEM and optical microscopy and determined the correct mixture of $B_2O_3$38-Sn62 wt% for surface texture.

- Experimental analyses of at least 60 samples conducted using different techniques and Pb-free materials (such as B_2O_3, Sn, Bi, and/or Zn) in combination with pure Sn solder wire and/or Sn90-In10 wt% alloy, among which five vacuum glazing samples of various designs and techniques discussed in this paper. The fusion edge-sealed vacuum glazing (sample 'A5'), constructed with bonded Sn62-$B_2O_3$38 wt% mixture for surface texture fused with Sn90-In10 wt% alloy at 450˚C, is amongst the successful design and construction method. The pump-out hole seal of fusion edge-sealed vacuum glazing is achieved at the hot-plate surface heat induction of 50±5˚C and the cavity vacuum pressure of $8.2 \cdot 10^{-4}$ Pa. In which, 20 trials of similar sample ('A5') having different sizes constructed verifies the persistent fusion edge-seal at the accuracy of 99.5% of cavity vacuum pressure.

- A validated three-dimensional finite element model employed and the U_c and U_t values of fusion edge-sealed vacuum glazing (sample 'A5'), area of 300·300mm with 10 mm wide fusion edge-seal, predicted to be 1.039 $Wm^{-2}K^{-1}$ and 1.4038 $Wm^{-2}K^{-1}$, respectively. The centre-of-pane and total thermal conductance values were predicted to be 1.24 $Wm^{-2}K^{-1}$ and 1.79 $Wm^{-2}K^{-1}$, respectively. The results implicate that the influence of edge effects is more in a small size vacuum glazing than in a larger vacuum glazing. Due to the use of a 10mm wide fusion seal, the edge effects can be seen to extend to a distance of up to 72mm and 45mm from the edge on the warm and cold side surfaces.

- The cost of the edge sealing materials for the construction of fusion edge-sealed vacuum glazing (sample 'A5') at the laboratory scale was calculated to be GBP 3.72 for the area of 300·300mm and GBP 10.56 for the area of 1000mm·1000mm, the cost of pump-out hole sealing is included. Comparing this to the predicted solder glass based samples 'A6' and 'A7' the fusion edge-sealed vacuum glazing reduces the cost to 75.8% and 86.84% respectively. Overall, it can be seen that the fusion edge-sealed vacuum glazing is seemed to be the most low-cost solution for mass production.

Acknowledgement

This work was supported by the Engineering and Physical Sciences Research Council (EPSRC) of the UK (EP/G000387/1).

Data Availability

In support of open access research, all supplementary data to this article is available and can be found online at:

[dataset] Memon S. Design, fabrication and performance analysis of vacuum glazing units fabricated with low and high temperature hermetic glass edge sealing materials (Doctoral dissertation, Loughborough University). https://dspace.lboro.ac.uk/2134/14562.

References

[1] Peng J, Yan J, Zhai Z, Markides CN, Lee ES, Eicker U, Zhao X, Kuhn TE, Sengupta M, Taylor RA. Solar energy integration in buildings. Applied Energy. 2020;264. https://doi.org/10.1016/j.apenergy.2020.114740.

[2] Chen S, Kharrazi A, Liang S, Fath BD, Lenzen M, Yan J. Advanced approaches and applications of energy footprints toward the promotion of global sustainability. Applied Energy. 2020;261. https://doi.org/10.1016/j.apenergy.2019.114415.

[3] Zhou N, Khanna N, Feng W, Ke J, Levine M. Scenarios of energy efficiency and CO 2 emissions reduction potential in the buildings sector in China to year 2050. Nature Energy. 2018 Nov;3(11):978-84. https://doi.org/10.1038/s41560-018-0253-6.

[4] Katsura T, Memon S, Radwan A, Nakamura M, Nagano K. Thermal performance analysis of a new structured-core translucent vacuum insulation panel in comparison to vacuum glazing: Experimental and theoretically validated analyses. Solar Energy. 2020 Mar 15;199:326-46. https://doi.org/10.1016/j.solener.2020.02.030.

[5] Memon S. Analysing the potential of retrofitting ultra-low heat loss triple vacuum glazed windows to an existing UK solid wall dwelling. International Journal of Renewable Energy Development (IJRED). 2014 Oct 15;3(3):161-74. https://doi.org/10.14710/ijred.3.3.161-174.

[6] Memon S, Eames PC. Predicting the solar energy and space-heating energy performance for solid-wall detached house retrofitted with the composite edge-sealed triple vacuum glazing. Energy Procedia. 2017 Sep 1;122:565-70. https://doi.org/10.1016/j.egypro.2017.07.419.

[7] Fang Y, Memon S, Peng J, Tyrer M, Ming T. Solar thermal performance of two innovative configurations of air-vacuum layered triple glazed windows. Renewable Energy. 2020 May 1;150:167-75. https://doi.org/10.1016/j.renene.2019.12.115.

[8] Memon S, Eames PC. Solar energy gain and space-heating energy supply analyses for solid-wall dwelling retrofitted with the experimentally achievable U-value of novel triple vacuum glazing. Journal of Daylighting. 2017 Jun;4(1):15-25. https://doi.org/10.15627/jd.2017.2.

[9] Radwan A, Katsura T, Memon S, Serageldin AA, Nakamura M, Nagano K. Thermal and Electrical Performances of Semi-Transparent Photovoltaic Glazing Integrated with Translucent Vacuum Insulation Panel and Vacuum Glazing. Energy Conversion and Management. 2020 Apr. https://doi.org/10.1016/j.enconman.2020.112920.

[10] Fang Y, Hyde TJ, Arya F, Hewitt N, Eames PC, Norton B, Miller S. Indium alloy-sealed vacuum glazing development and context. Renewable and Sustainable Energy Reviews. 2014 Sep 1;37:480-501. https://doi.org/10.1016/j.rser.2014.05.029.

[11] Collins RE, Simko TM. Current status of the science and technology of vacuum glazing. Solar Energy. 1998 Mar 1;62(3):189-213. https://doi.org/10.1016/S0038-092X(98)00007-3.

[12] Memon S, Fang Y, Eames PC. The influence of low-temperature surface induction on evacuation pump-out hole sealing and thermal performance of composite edge sealed vacuum insulated glazing. Renewable energy. 2019 May 1;135:450-64. https://doi.org/10.1016/j.renene.2018.12.025.

[13] Robinson SJ, Collins RE. Evacuated windows-theory and practice. InISES solar world congress, international solar energy society, Kobe, Japan 1989 Sep.

[14] Collins RE, Robinson SJ. Evacuated glazing. Solar Energy. 1991 Jan 1;47(1):27-38. https://doi.org/10.1016/0038-092X(91)90060-A.

[15] Collins RE, Robinson SJ, inventors; University of Sydney, assignee. Thermally insulating glass panel and method of construction. United States patent US 5,657,607. 1997 Aug 19.

[16] Eames PC. Vacuum glazing: Current performance and future prospects. Vacuum. 2008 Mar 14;82(7):717-22. https://doi.org/10.1016/j.vacuum.2007.10.017.

[17] Ogunseitan OA. Public health and environmental benefits of adopting lead-free solders. Jom. 2007 Jul 1;59(7):12-7. https://doi.org/10.1007/s11837-007-0082-8.

[18] Griffiths PW, di Leo M, Cartwright P, Eames PC, Yianoulis P, Leftheriotis G, Norton B. Fabrication of evacuated glazing at low temperature. Solar Energy. 1998 Oct 1;63(4):243-9. https://doi.org/10.1016/S0038-092X(98)00019-X.

[19] Memon S, Farukh F, Eames PC, Silberschmidt VV. A new low-temperature hermetic composite edge seal for the fabrication of triple vacuum glazing. Vacuum. 2015 Oct 1;120:73-82. http://dx.doi.org/10.1016/j.vacuum.2015.06.024.

[20] Memon S. Experimental measurement of hermetic edge seal's thermal conductivity for the thermal transmittance prediction of triple vacuum glazing. Case studies in thermal engineering. 2017 Sep 1;10:169-78. https://doi.org/10.1016/j.csite.2017.06.002.

[21] Weston GF. Ultrahigh vacuum practice. Elsevier; 2013 Oct 22.

[22] Katz H, inventor; Siemens AG, assignee. Vacuum-tight carbon bodies. United States patent US 3,878,425. 1975 Apr 15.

[23] Mientkewitz G, Schaffrath W, Köhler T, inventors; NARVA Lichtquellen GmbH and Co KG, assignee. Glass-metal connection, in particular for a vacuum-tube solar collector. United States patent US 8,097,318. 2012 Jan 17.

[24] Frieser RG. A review of solder glasses. Active and Passive Electronic Components. 1975;2(3):163-99. https://doi.org/10.1155/APEC.2.163.

[25] GALLUP J. Properties of low-temperature solder glasses. Celam. Bull.. 1957;36:47-51.

[26] Roth A. Vacuum sealing techniques. Springer Science & Business Media; 1994.

[27] Kohl WH. Handbook of Materials and Techniques for Vacuum Devices, Reinhold Pub. Corp., New York, NY. 1967.

[28] Donald IW. Preparation, properties and chemistry of glass-and glass-ceramic-to-metal seals and coatings. Journal of materials science. 1993 Jan 1;28(11):2841-86. https://doi.org/10.1007/BF00354689.

[29] Uhlmann D, editor. Elasticity and Strength in Glasses: Glass: Science and Technology. Elsevier; 2012 Dec 2.

[30] Turner GM, Collins RE, Facer GR, Sheumack MA. Outgassing effects in evacuated glazing. In Optical Materials Technology for Energy Efficiency and Solar Energy Conversion XIII 1994 Sep 9 (Vol. 2255, pp. 660-672). International Society for Optics and Photonics. https://doi.org/10.1117/12.185407.

[31] Lewin G. Fundamentals of vacuum science and technology.

[32] Norman NC, editor. Chemistry of arsenic, antimony and bismuth. Springer Science & Business Media; 1997 Dec 31.

[33] McCulloch L. A crystalline boric oxide. Journal of the American Chemical Society. 1937 Dec;59(12):2650-2.

[34] Woods WG. An introduction to boron: history, sources, uses, and chemistry. Environmental health perspectives. 1994 Nov;102(suppl 7):5-11. https://doi.org/10.1289/ehp.94102s75.

[35] ASTM. Standard definitions of Terms relating to Glass and Glass Products, Standard C, 162-52/56.

[36] Winter A. Glass formation. Journal of the American Ceramic Society. 1957 Feb;40(2):54-8. https://doi.org/10.1111/j.1151-2916.1957.tb12574.x.

[37] Murabayashi H, Kawakita K, Nakamura K, Kobatake S, inventors; Toshiba Corp, assignee. Bismuth-tin-indium alloy. United States patent US 4,214,903. 1980 Jul 29.

[38] Dumesnil ME, Schreier U, inventors; Technology Glass Corp, assignee. Lead-zinc-boron sealing glass compositions. United States patent US 3,963,505. 1976 Jun 15.

[39] Kawamura S, Yamaguchi F, inventors; Nippon Electric Glass Co Ltd, assignee. Glass solder. United States patent US 3,645,761. 1972 Feb 29.

[40] Ide A, inventor; Asahi Techno Glass Corp, assignee. Low melting glass, sealing composition and sealing paste. United States patent US 7,291,573. 2007 Nov 6.

[41] Schwarz-Schampera U, Herzig PM. Indium: Geology, mineralogy, and economics. Springer Science & Business Media; 2002 Apr 24.

[42] Maness LV. Predicting indium and tellurium availability. In2010 35th IEEE Photovoltaic Specialists Conference 2010 Jun 20 (pp. 000560-000613). IEEE. https://doi.org/10.1109/PVSC.2010.5616838.

[43] [dataset] Memon S. Design, fabrication and performance analysis of vacuum glazing units fabricated with low and high temperature hermetic glass edge sealing materials (Doctoral dissertation, Loughborough University). https://dspace.lboro.ac.uk/2134/14562.

[44] Collins RE, Fischer-Cripps AC, Tang JZ. Transparent evacuated insulation. Solar Energy. 1992 Nov 1;49(5):333-50. https://doi.org/10.1016/0038-092X(92)90106-K.

[45] Fischer-Cripps AC, Collins RE, Turner GM, Bezzel E. Stresses and fracture probability in evacuated glazing. Building and environment. 1995 Jan 1;30(1):41-59. https://doi.org/10.1016/0360-1323(94)E0032-M.

[46] Lenzen M, Collins RE. Long-term field tests of vacuum glazing. Solar Energy. 1997 Jul 1;61(1):11-5. https://doi.org/10.1016/S0038-092X(97)00038-8.

[47] Wang J, Eames PC, Zhao JF, Hyde T, Fang Y. Stresses in vacuum glazing fabricated at low temperature. Solar energy materials and solar cells. 2007 Feb 15;91(4):290-303. https://doi.org/10.1016/j.solmat.2006.10.007.

[48] Wullschleger L, Manz H, Wakili KG. Finite element analysis of temperature-induced deflection of vacuum glazing. Construction and Building Materials. 2009 Mar 1;23(3):1378-88. https://doi.org/10.1016/j.conbuildmat.2008.07.010.

[49] Fang Y, Eames PC, Norton B, Hyde TJ. Experimental validation of a numerical model for heat transfer in vacuum glazing. Solar Energy. 2006 May 1;80(5):564-77. https://doi.org/10.1016/j.solener.2005.04.002.

[50] Fang Y, Eames PC, Hyde TJ, Norton B. Complex multimaterial insulating frames for windows with evacuated glazing. Solar energy. 2005 Sep 1;79(3):245-61. https://doi.org/10.1016/j.solener.2004.11.009.

[51] ASTM. Standard procedures for determining the steady state thermal transmittance of fenestration systems, ASTM Standard E 1423-91, in: Annual Book of ASTM Standard 04.07, 1994, pp. 1160–1165.

[52] Fang Y, Hyde T, Hewitt N, Eames PC, Norton B. Comparison of vacuum glazing thermal performance predicted using two-and three-dimensional models and their experimental validation.

Solar Energy Materials and Solar Cells. 2009 Sep 1;93(9):1492-8.
https://doi.org/10.1016/j.solmat.2009.03.023.
[53] Memon S, Farukh F, Kandan K. Effect of cavity vacuum pressure diminution on thermal performance of triple vacuum glazing. Applied Sciences. 2018 Sep;8(9):1705. https://doi.org/10.3390/app8091705.
[54] Zhao JF, Eames PC, Hyde TJ, Fang Y, Wang J. A modified pump-out technique used for fabrication of low temperature metal sealed vacuum glazing. Solar Energy. 2007 Sep 1;81(9):1072-7. https://doi.org/10.1016/j.solener.2007.03.006.
[55] Garrison JD, Collins RE. Manufacture and cost of vacuum glazing. Solar Energy. 1995 Sep 1;55(3):151-61. https://doi.org/10.1016/0038-092X(95)00046-T.
[56] McSporran N. Properties and performance of vacuum insulated glazing. Journal of Green Building. 2014 Apr;9(1):60-74. https://doi.org/10.3992/1943-4618-9.1.60.
[57] Courtesy by McSporran, Neil. Cost per m2 of the Specia-vacuum glazing, Pilkington North America, 2013, Inc, 811 Madison Avenue, Toledo, Ohio.

Highlights

- Novel concept of forming glass-metallic textured layer for hermetic fusion seal.
- Fusion edge-seal invented when Sn62-$B_2O_3$38 wt% fused with Sn90-In10 wt% alloy.
- Fusion edge-sealed vacuum glazing (FSVG) achieved vacuum pressure of $8.2 \cdot 10^{-4}$ Pa.
- Validated FEM predicted central thermal performance of FSVG to be 1.039 $Wm^{-2}K^{-1}$.
- FSVG is cost-effective, ultrasonic-soldering free and Pd-free solution.

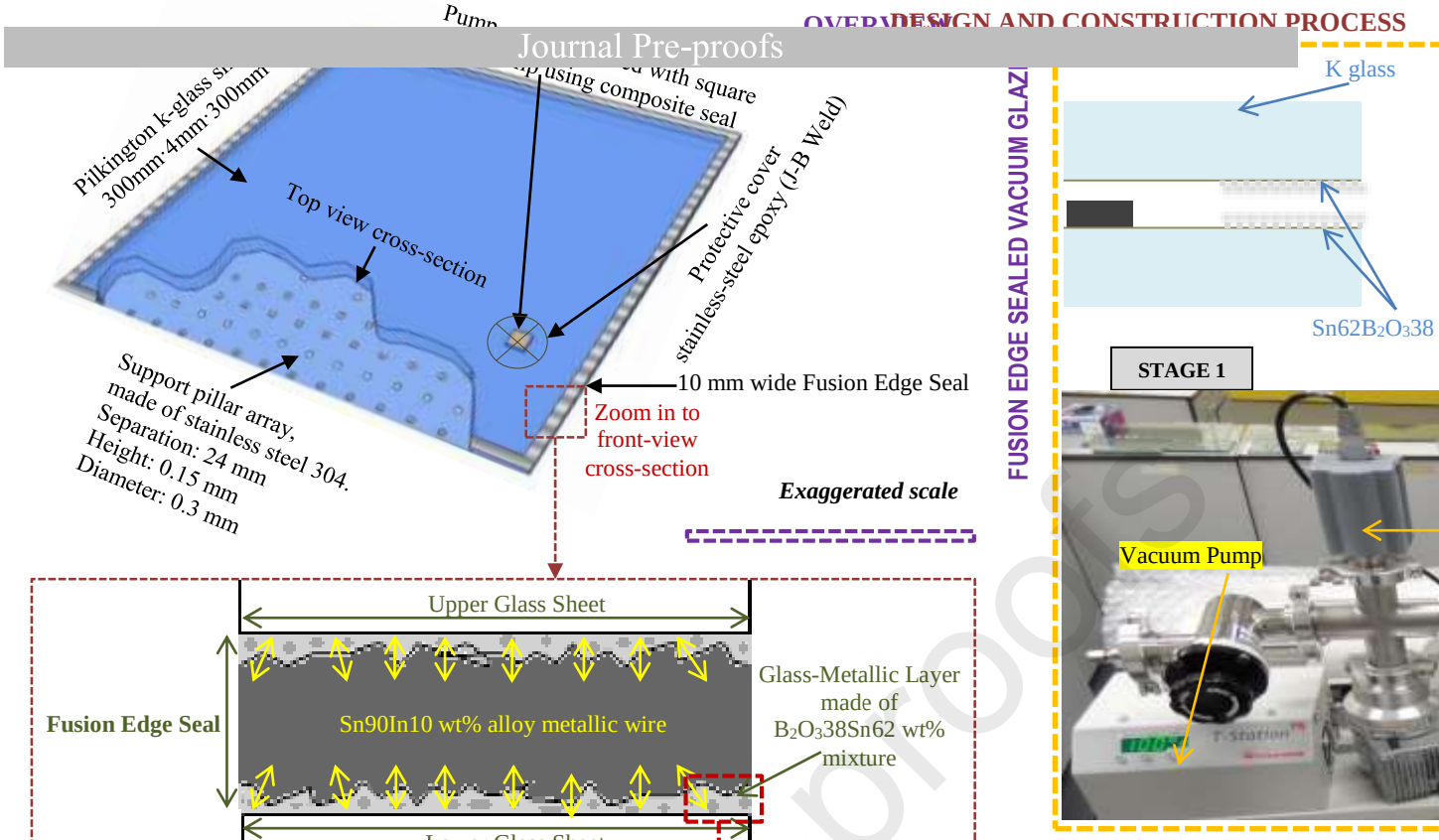

VACUUM PRESSURE AND THERMAL PERFORMANCE ANALYSES

MICROSTRUCTURAL ANALYSES

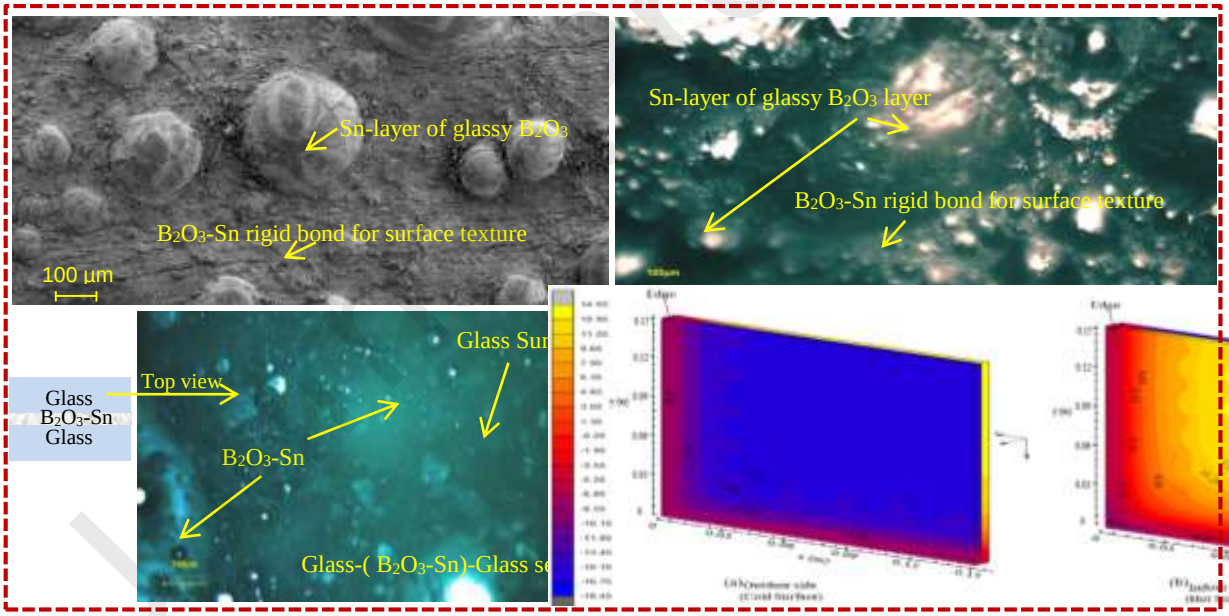

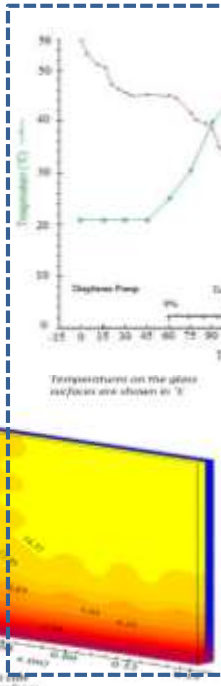

CRediT Author Statement

Saim Memon: Term, Conceptualisation, Methodology, Software, Validation, Formal Analysis, Investigation, Data Curation, Writing-Original Draft, writing-Review & Editing, Visualisation.
Philip C. Eames: Supervision, Conceptualization, Reviewing-Editing,